AD-A125 622 DESIGN AND EVALUATION OF CASCADE TEST FACILITY(U) AIR FORCE INST OF TECH WRIGHT-PATTERSON AFB OH SCHOOL OF ENGINEERING D M ALLISON JUN 82 AFIT/GAE/AA/81D-2 1/1

UNCLASSIFIED F/G 20/4 NL

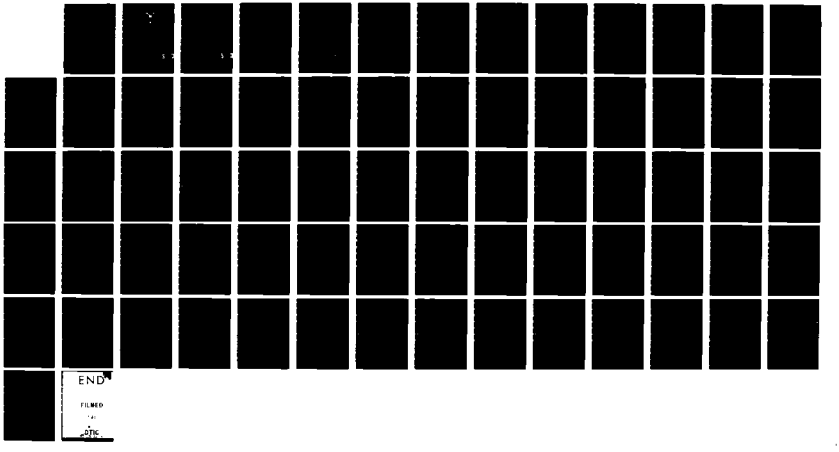

END

FILMED

DTIC

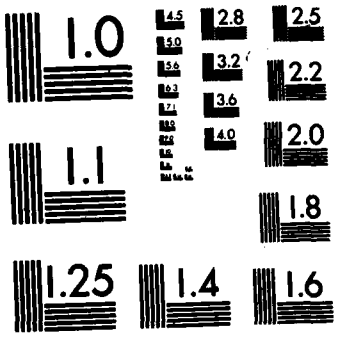

DESIGN AND EVALUATION OF A CASCADE TEST FACILITY

THESIS

AFIT/GAE/AA/81D-2

Dennis M. Allison
Capt USAF

DEPARTMENT OF THE AIR FORCE
AIR UNIVERSITY (ATC)
AIR FORCE INSTITUTE OF TECHNOLOGY

Wright-Patterson Air Force Base, Ohio

AFIT/GAE/AA/81D-2

DESIGN AND EVALUATION OF A CASCADE TEST FACILITY

THESIS

AFIT/GAE/AA/81D-2 Dennis M. Allison
Capt USAF

AFIT/GAE/AA/81D-2

DESIGN AND EVALUATION OF A CASCADE TEST FACILITY

THESIS

Presented to the Faculty of the School of Engineering

of the Air Force Institute of Technology

Air University

in Partial Fulfillment of the

Requirements for the Degree of

Master of Science

by

Dennis M. Allison, B.S.

Capt USAF

Graduate Aeronautical Engineering

June 1982

Acknowledgments

I wish to thank the members of my thesis committee, Dr. Harold E. Wright, Dr. Peter J. Torvik, and especially my principal advisor, Dr. William C. Elrod, for the guidance and support they gave me on this project. I also thank Major John Vonada for his many valuable suggestions, and Mr. Leroy Cannon and Mr. William Baker for their technical support. Thanks are also due to the men of the AFIT Fabrication Branch, who did a truly superior job of building the various components of the Cascade Test Facility.

Dennis M. Allison

Contents

List of Figures

List of Symbols

A	Area
a	Distance from leading edge to point of maximum thickness
c	Chord
DC	Direct current
F	Degrees Fahrenheit
g	Gravitational constant
l	length
lb_m	Pounds mass
m	Slope of sensor calibration curve
$\dot{m}$	Mass flow rate
P	Static pressure
P_t	Total pressure
PE	Ejector total pressure
psia	Pounds per square inch absolute
psig	Pounds per square inch gauge
R	Gas constant
Re	Reynolds number
RMS	Root mean square
S	Blade spacing
T	Static temperature
T_t	Total temperature
TCF	Temperature correction factor
V	Velocity
V_{fluc}	Fluctuating velocity
V_{max}	Maximum velocity in flow field

v	Voltage
v_{RMS}	Root mean square voltage
γ	Specific heat ratio
δ	Boundary layer thickness
δ^*	Gas deviation angle
θ	Camber angle
μ	Coefficient of absolute viscosity
ν	Coefficient of kinematic viscosity
ρ	Air density

Abstract

A cascade test facility was designed and built. The facility delivers 4.0 lb_m/sec of air to the test section with turbulence intensities of 2.1 percent. The maximum Reynolds number observed was 3.24 X 10^6 per foot.

The velocity and turbulence intensity profiles in the flow stream behind the blades were investigated with a hot film anemometer. The fluid turning angle was 30 degrees. The profiles were obtained at .5, 2, and 4 chord lengths downstream from the trailing edges at Reynolds numbers of 2.34, 2.83, and 2.97 million per foot. The profiles behind the three center blades of the five blade cascade were very closely matched in all test cases. A flow tuning adjustment in the test section requires redesign; otherwise, the facility is adequate for the testing of compressor and turbine cascades.

I. Introduction

Background

The testing of axial flow compressor and turbine blades is normally accomplished in a two dimensional cascade. Cascade testing allows the gathering of a great deal of data that can be used in engine design work. Specifically, the effects of blade shape, geometry, and surface roughness can be determined by studying the wakes of cascaded blades. It was in support of two such studies, both under the sponsorship of the Air Force Wright Aeronautical Laboratories Aero Propulsion Laboratory, that the AFIT Cascade Test Facility (CTF) was designed and built. The first study was a Ph.D. dissertation investigating the mixing process behind compressor blades with crenelated trailing edges (Ref. 1); the second concerned the effect of surface roughness on compressor blade performance (Ref. 2). These studies strongly influenced the design, but care was taken to ensure that the facility could be adapted to other studies at a later time.

Objectives and Scope

Ideally, the design of the CTF would be flexible enough to permit its use both as a cascade test facility and as a conventional wind tunnel. To achieve the required flexibility the test section was to allow investigation of compressor and turbine blade cascades with the cascade geometry and blade profile, surface roughness, and trailing edge configuration as possible variables. The compressor blade studies mentioned above dictated the principal design goal of achieving a Reynolds number (Re) of 3.0×10^6 per foot. Sufficient mass flow was required to support a test section large enough so that wall effects did not invalidate the

data. The objectives of this thesis, then, were to design and build a wind tunnel in which cascade testing could be done, to design and build a suitable test section which would simulate operation of an infinite cascade, and to test the entire apparatus to determine its performance and acceptability.

II. Facility Design

The initial effort of this study consisted of the design of the facility. The CTF is composed of three major elements: 1) the flow supply system, 2) the diffuser/stilling chamber and 3) the test section, including associated data gathering equipment.

Air Supply System

The air used in the CTF is obtained from two completely independent sources: a centrifugal blower and a high pressure augmentor/ejector. The 40 horsepower centrifugal blower has a nameplate rating of 3000 cubic feet per minute at 26 ounces of head, and accounts for the majority of the available mass flow. The entire blower assembly is enclosed in a foam padded box which suppresses motor and compressor noise and allows the intake air to be channeled through an electronic air cleaner. Flow to the blower is normally obtained through a 12 in. duct from outside the building. Outside air is used because the test section exhausts into the laboratory, and heating of the air by the blower appreciably increases the room temperature after long periods of blower operation. A significant benefit is realized by using the cooler outside air, especially in the winter months, since this increases the fluid density and therefore the Reynolds number. This increase in density is on the order of 10 percent if air at 30 F is used rather than air at 80 F.

The blower is not capable of providing sufficient mass flow and pressure to achieve the design Reynolds number. For this reason, compressed air from the laboratory high pressure air supply is injected into the blower discharge air. Nominal maximum delivery is 1.0 lb_m/sec

at 100 psia. The ejector design is based on the work of Keenan, Neumann, and Lustwerk (Refs. 3,4), and is shown schematically in Fig. 1. The

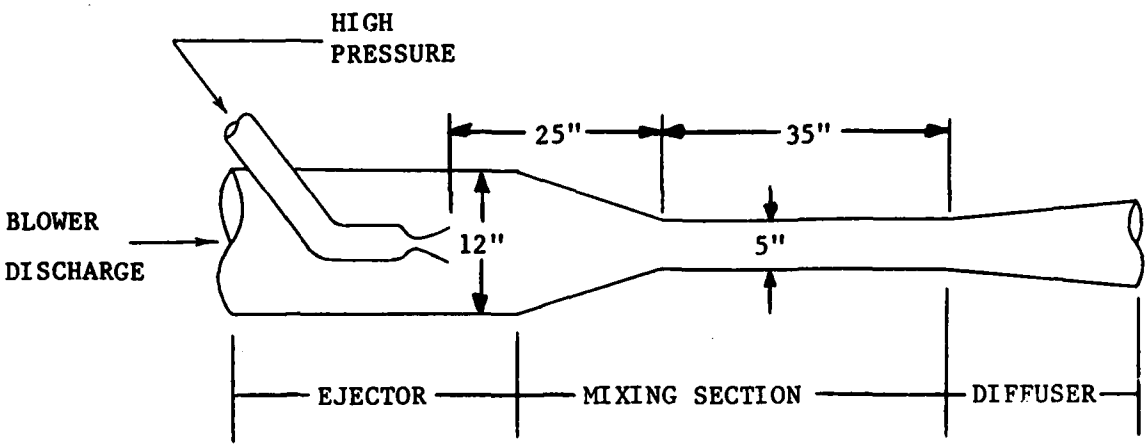

Figure 1. Ejector Schematic

ejector nozzle can be used as either a converging or converging-diverging nozzle, as the diverging portion is attached by screw threads and is easily removed. Also, while the CTF was designed to be operated with the ejector and blower both running, this is not necessary. At an ejector total pressure (PE) of 80 psig, the ejector alone produces a tank pressure of approximately 40 in. of water, which is the same as the tank pressure for blower only operation. Thus a continuous range of flow conditions from zero flow to the maximum capacity of the facility is possible.

Diffuser/Stilling Chamber

Upon departure from the ejector mixing section, the flow enters a 9 foot long diffusing section which slows the flow velocity to approximately 20 ft/sec. The divergence half angle is 7 degrees. The flow is then radially diffused by means of a center body plug at the beginning

of the stilling chamber tank. See Fig. 2. In addition to aiding the diffusion process, the plug also interferes with the acoustic path between

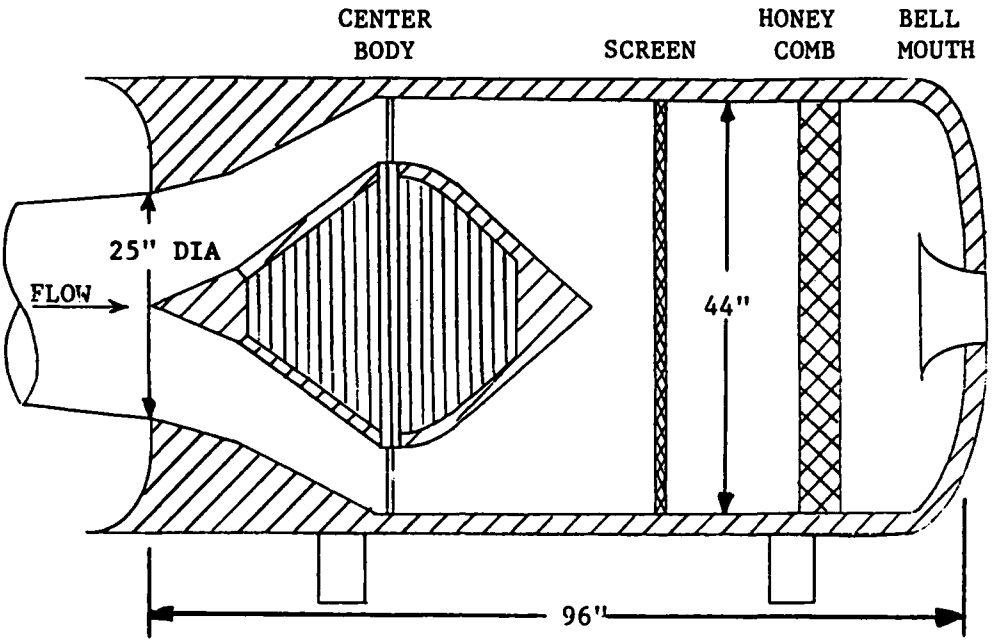

Figure 2. Stilling Chamber Schematic

the air supply system and the test section. The plug is built of styrofoam covered with two inch thick foam rubber. The outer annulus corresponding to the center body is made of contoured foam rubber. The effective divergence half angle is 4.84 degrees. At the exit plane of the cone, the flow velocity is approximately 10 ft/sec. The flow then passes through one layer of 40 mesh wire screen which traps particulate matter and provides a slight back pressure along the divergent portion of the center body. Finally, the flow encounters a 4 in. thick honeycomb grid which straightens the flow prior to its entry into the test section.

Test Section Design

Determination of Mass Flow Capabilities. Before the size of the test section could be established it was necessary to determine how much air the flow supply system could furnish. This was established by running the supply system with various sized square-edged orifices bolted to the exit of the stilling chamber. Pitot-static traverses were then made to determine the location and size of the vena contractae at several ejector pressures. The initial runs were accomplished with the ejector operating in both the converging and converging-diverging configurations. No appreciable difference in tank total pressure was noted between the two configurations. Since the total pressure achieved was adequate to produce the required Reynolds number, no further attempt was made to optimize ejector performance. The ejector was operated in the converging-diverging mode for the remainder of the study. The measured diameters of the vena contractae were used to compute the effective exit areas, and these areas were plotted versus tank total pressure with ejector pressure as a parameter.

Figure 3 shows the variation of pressure recovery with exit area. It is obvious that the maximum pressure recovery is achieved for an exit area of between 15 and 16 sq in. Note that at higher ejector pressures, the performance of the system falls off rapidly as the exit area is decreased below 12 sq in. This is attributed to blower stall due to the increased pressure in the stilling chamber as a result of ejector operation. This effect is much more pronounced at higher ejector pressures; since the facility normally operates under these conditions, the optimum exit area was found to be 16 sq in.

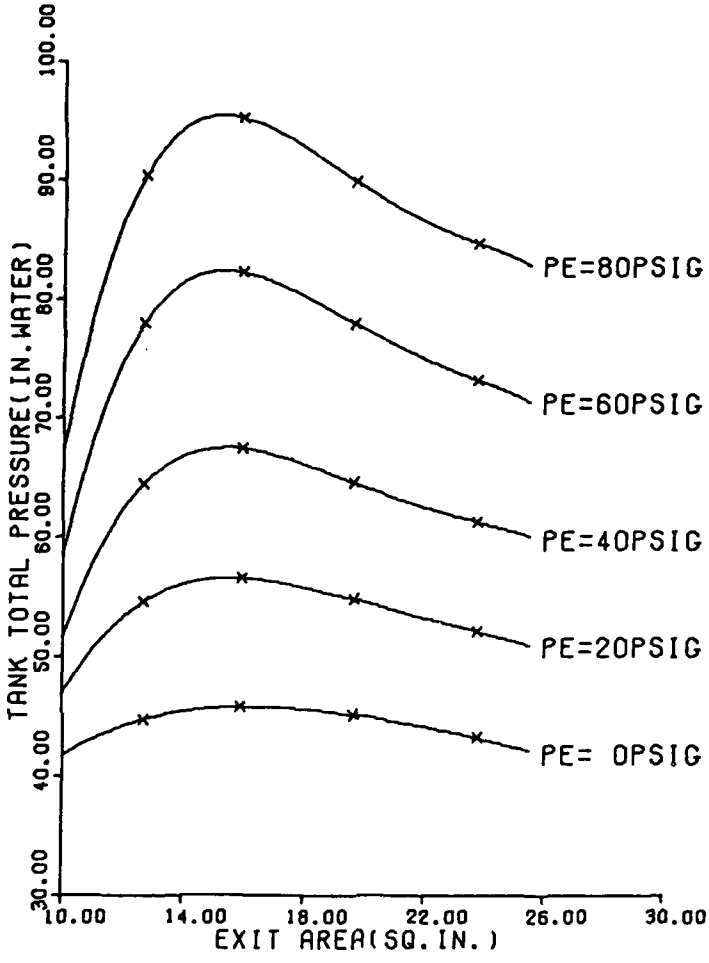

Figure 3. Variation of Pressure Recovery with Stilling Chamber Exit Area Using Square Edge Orifices

Cascade Test Section Design Considerations. In addition to the basic design goal of achieving a Reynolds number of 3.0 X 10^6 per foot, there are several other factors which influence the design of the test

section to be employed. These are discussed in detail below.

1). The size of the test section must be such that wall effects do not invalidate the data. Therefore, the width must be great enough so that the boundary layers do not extend to the center line of the test section. The boundary layer thickness was estimated by means of the turbulent flow boundary layer thickness equation (Ref. 5:42)

$$\frac{\delta}{x} = 0.37\left[\frac{V\,x}{\nu}\right]^{-.2} \qquad (1)$$

For $x = 3$ ft, $V = 300$ ft/sec, $\nu = 1.5 \times 10^{-4}$ ft^2/sec, the boundary layer thickness $\delta = 0.59$ in. This equation only applies to turbulent flow over a flat plate at zero incidence. However, Schlichting points out (Ref. 5:511) that the centrifugal forces acting on a fluid traversing a convex surface impede transverse motions within the fluid. This tends to suppress mixing, resulting in a thinner boundary layer. Schlichting also points out that wall curvature has little effect on boundary layer stability if the boundary layer thickness is much less than the radius of curvature. Therefore, considering the bell mouth inlet to be a flat plate is a conservative assumption, and leads to a minimum test section width greater than $2 \times 0.59 = 1.18$ in. With this in mind, the test section width was chosen to be 2 in; this set the test section height at 8 inches to provide an exit area of 16 sq in.

2). A typical cascade assembly for evaluation of compressor blade performance is shown in Fig. 4. In order to permit varying the angle of attack for a given cascade or varying the cascade geometry, an adjustable inlet bell mouth was provided at the exit of the stilling chamber.

The upper surface of the inlet could be adjusted to control the test section inlet area, as shown by the dashed lines in Fig. 5. The curvature of the bell mouth walls is that of an ASME long radius bell mouth. The effect of angle of attack on the channel height (and area) for a fixed cascade geometry is shown in Fig. 6.

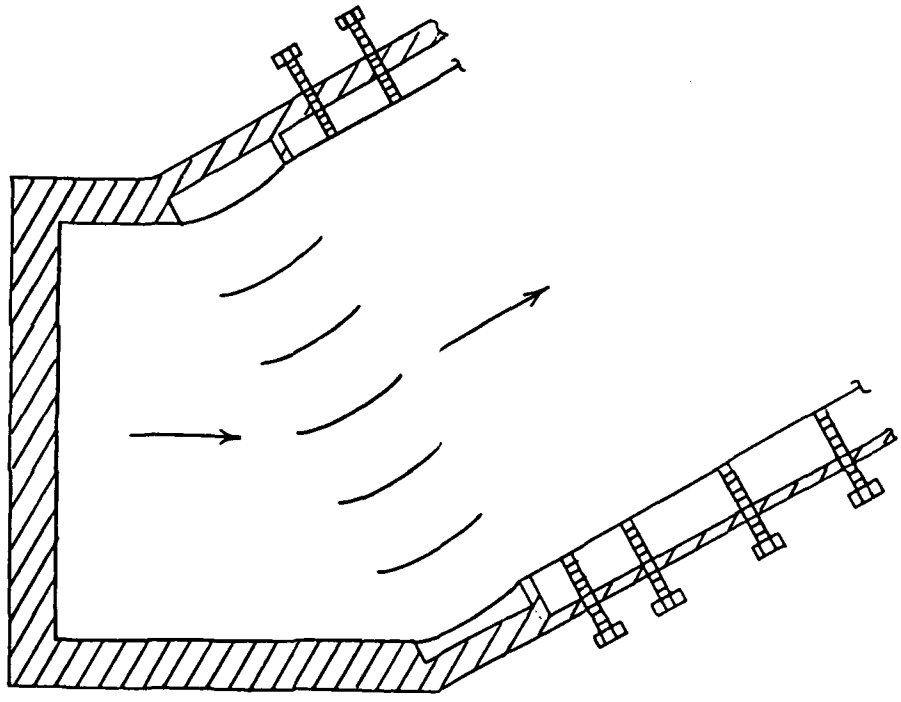

Figure 4. Test Section Schematic (Side View)

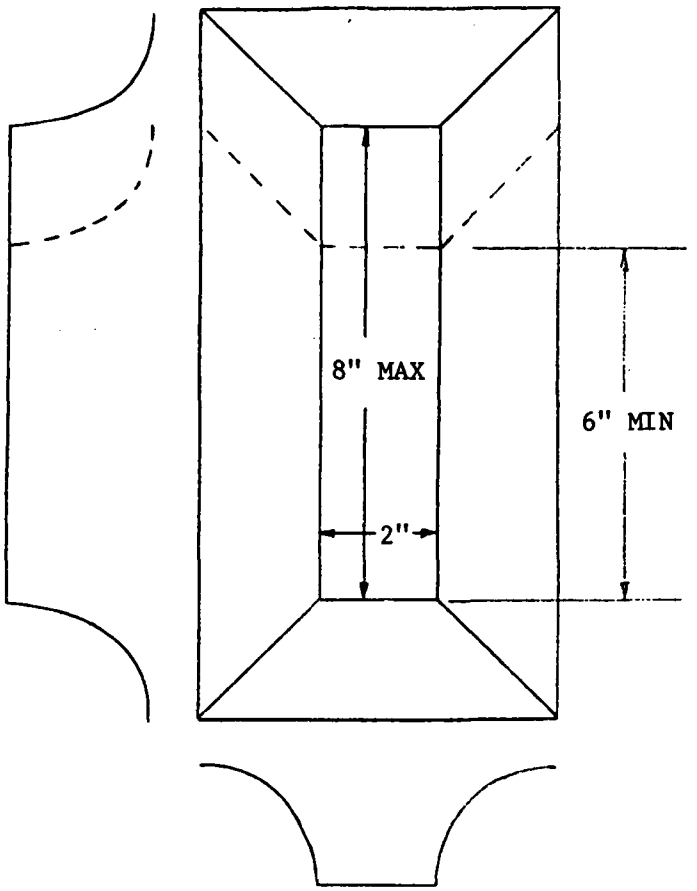

Figure 5. Test Section Inlet, Looking Downstream

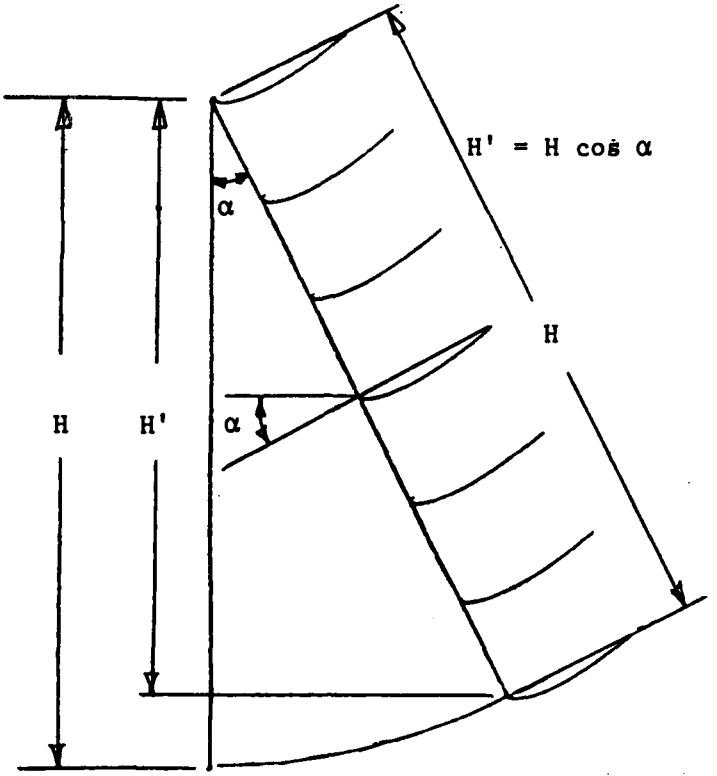

Figure 6. Variation of Test Section Frontal Area with Angle of Attack

3). Flexible end walls are used as a means of controlling the flow conditions downstream of the blades (Ref. 6). As shown in Fig. 4, these walls are driven by jack screws and held in place by the screws and by friction from the plexiglass side walls. The edges are sealed with rubber gasket material to prevent leakage. The walls may be used to adjust downstream flow direction and to vary the back pressure on the cascade. In addition, the effect of blade and/or cascade geometry on the performance of a diffuser located downstream of the blades may be investigated.

4). A flow traversing system designed to accommodate a pitot tube or a hot wire/hot film anemometer sensor was fabricated. The traverser was to be automated and capable of interfacing with the Hewlett-Packard

Automatic Data Acquisition System. The anemometer sensor was supported in the flow by an 18 in. probe support. The traverser permits probing the entire flow field from 1/2 in. behind the blade leading edges to the exit of the test section. A NACA 66-007 airfoil was used as a fairing around the probe support. See Fig. 7. This assembly is attached to the traversing system, which is driven in the streamwise (x) and vertical (z) directions by digital stepping motors. (The cascade coordinate system is shown in Fig. 8). The probe is positioned in the spanwise direction by a manually operated traverser. Probe location is read from a digital position indicator with resolutions of .001 in. in the vertical direction and .002 in. in the streamwise direction. Details concerning the collection and reduction of data are included in Appendix A.

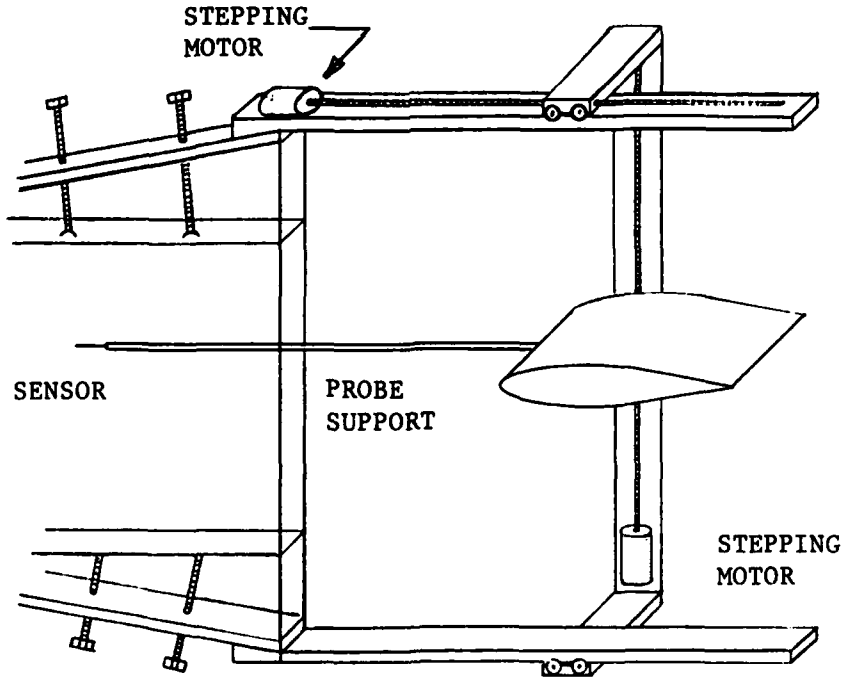

Figure 7. Test Section Traversing System

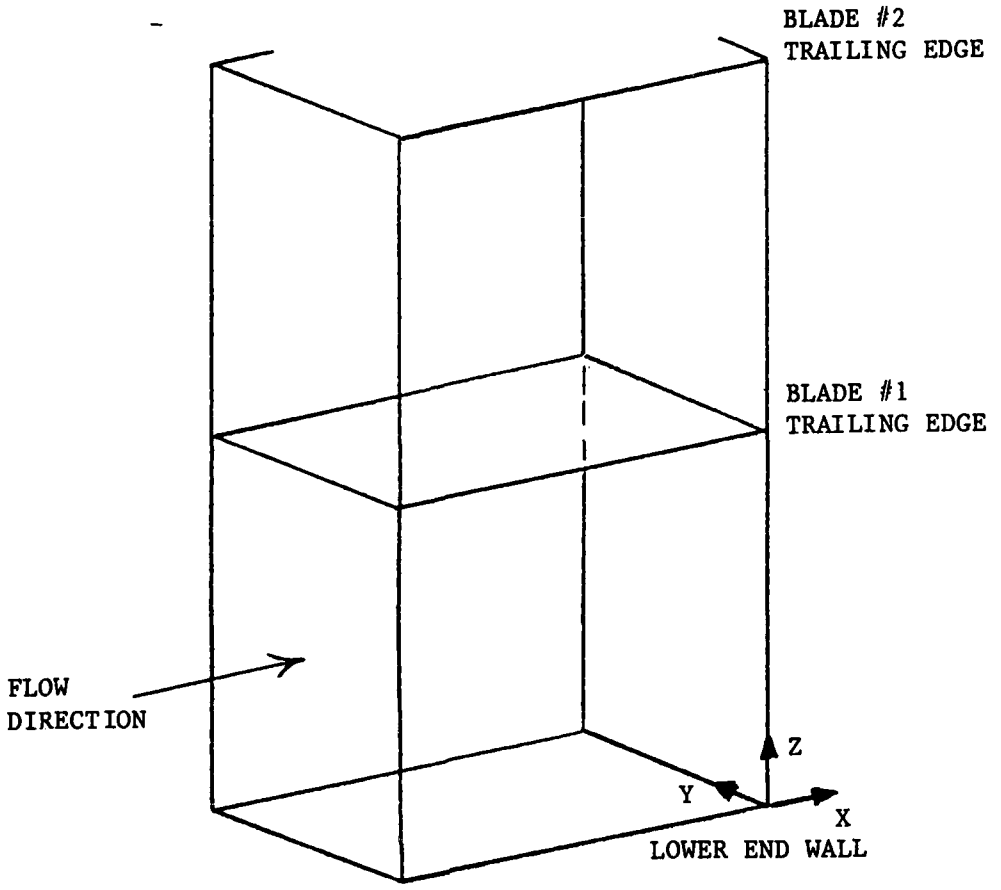

Figure 8. Cascade Coordinate System

5). Ease of access to the blades was an important consideration to permit adjustments to or changing of the blades. The test section side walls were built of plexiglass, and the blades were secured by means of pins which mated with holes in the side walls. This adequately supported the blades, and allowed the walls to be easily removed. This system also has the advantage that schlieren photographic studies of the test section flow conditions may be made.

6). In order to evaluate the performance of the CTF, a test section with cascade characteristics representative of an actual aircraft compressor was chosen. The blade chosen was a 2 dimensional model of a typical exit guide vane. A NACA 64-series airfoil with design lift

coefficient of 0.9 and thickness of 5.5 percent was chosen. The blades were cast of epoxy, both for ease of fabrication and ease of modifying the trailing edges. The profile coordinates were generated using a computational aerodynamics program, ICAAP (Ref. 7). An aspect ratio (span-to-chord) of 1.0 and a solidity (chord-to-spacing) of 1.5 were selected (Ref. 8). These two parameters, along with the previously selected width (span) and test section height required a chord of 2 in. and a blade spacing of 1.333 in. This geometry yielded an 8 inch five blade cascade. A blade was also half buried in each end wall to aid in simulating an infinite cascade. Thirty degrees was selected as the turning angle for the initial development phase. The blade orientation was set taking into account the gas deviation angle at the exit of the cascade (Ref. 9).

$$\delta^* = 0.26\theta\sqrt{S/c}\,[1-3(1-2a/c)] \qquad (2)$$

where θ = camber angle
S = blade spacing
c = chord
a = distance from leading edge to the point of maximum thickness

For the given blade and geometry, $\delta^* = 2.3$ degrees.

III. Facility Performance

The performance of the CTF was evaluated in two phases. First, the flow in the stilling chamber exit plane was studied with the test section removed to determine velocity and turbulence intensity levels in both the y and z planes. (Turbulence intensity is the ratio of the fluctuating (root mean square) velocity at a point to the maximum velocity in the flow field). Then the test section was installed and wake velocity and turbulence intensity profiles were obtained at three Reynolds numbers.

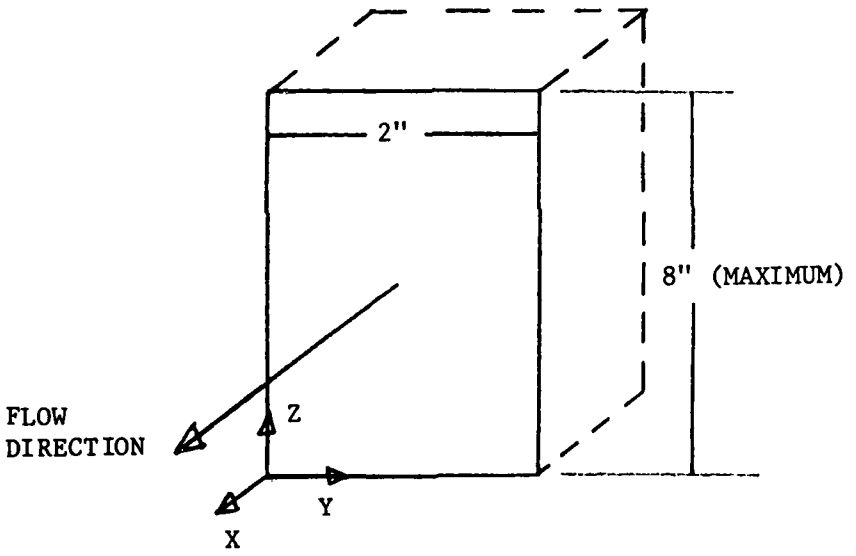

Figure 9. Stilling Chamber Exit Plane Coordinate System

Stilling Chamber Exit Plane Survey

The objective of the exit plane survey was to evaluate the characteristics of the flow provided by the air supply system without a test section installed. A uniform flow field upstream of the cascade was necessary in order to obtain valid data; it was assumed that installing

the test section would not seriously degrade the flow uniformity along the center line of the cascade. A traversing system using three manually operated mutually perpendicular traversers was bolted to the stilling chamber, and a TSI 1214-20 hot film sensor was used to measure velocity and turbulence intensity profiles in the exit plane.

The initial series of traverses was made in the vertical (z) plane at various distances from the side walls, with the flow channel height set at 8 in. These traverses indicated a pronounced anomaly in the flow field. The center of the disturbance was located approximately 0.75 in. from the upper end wall. The effect was present on both side walls and increased in severity approaching the side walls. When the channel height was reduced to 7.25 in., the disturbance center remained 0.75 in. from the upper wall. See Figs. 10-13. The flow defect was traced to the seam between the moveable wall of the bell mouth and the fixed side walls not having been sealed. As the flow accelerated through the bell mouth, the static pressure decreased, creating a pressure differential across the unsealed seam. This caused a thin jet to be injected along both side walls, severely disturbing the flow. The problem was solved by sealing the seam with a silicone based adhesive. Figures 14 and 15 show typical velocity and turbulence intensity profiles after the seam was sealed. Care must be taken to prevent such leaks when the bell mouth is readjusted, as the presence of such a disruption in the flow would invalidate any cascade data.

The next set of traverses was made in the horizontal (y) plane at various Reynolds numbers. Typical profiles are shown in Fig. 16, and indicate that the flow is uniform in the spanwise direction.

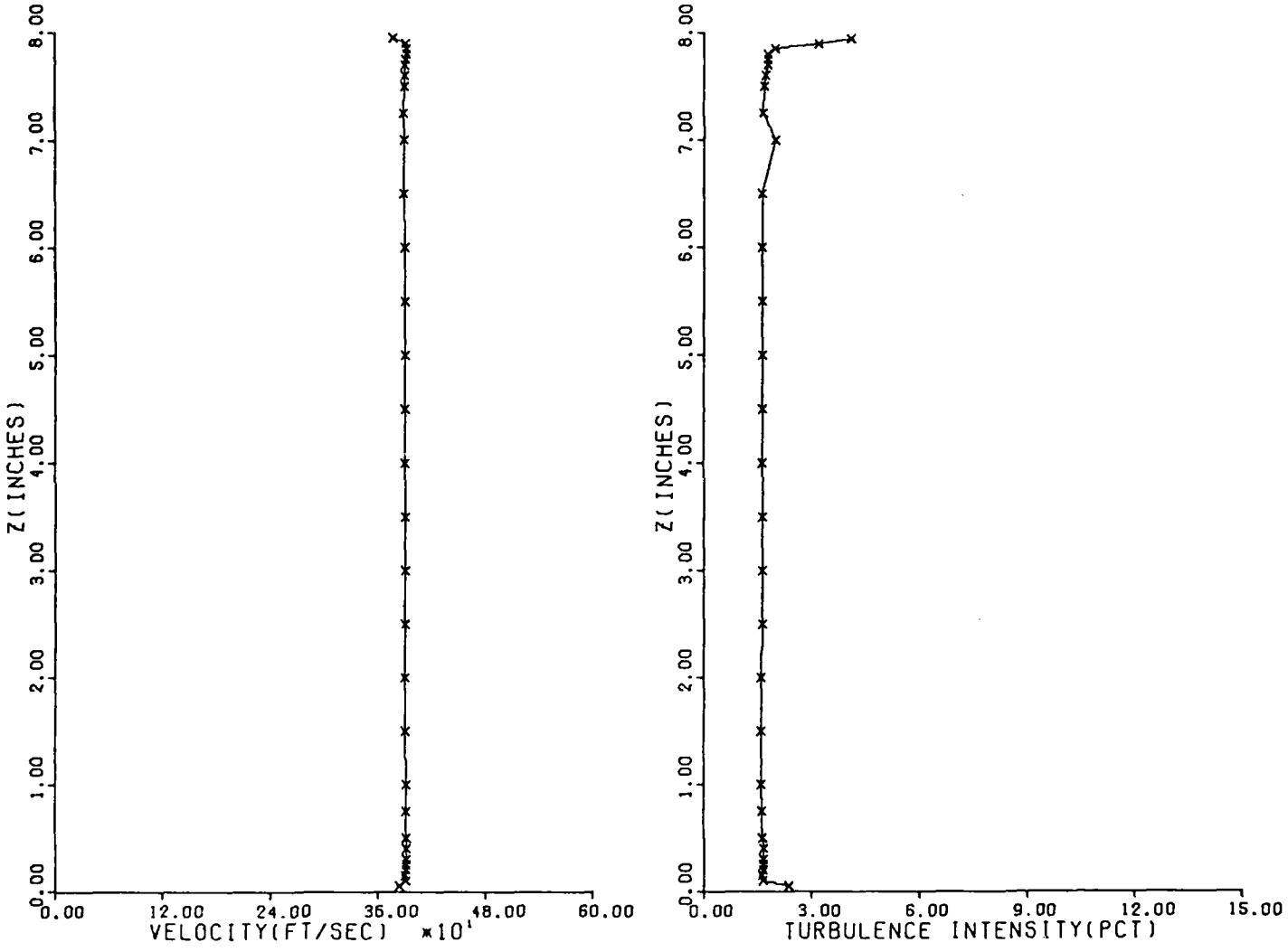

Figure 10. Velocity and Turbulence Intensity Profiles in the Stilling Chamber Exit Plane Bell Mouth Not Sealed, Y = 1.0 in., Exit Area = 16 Sq In.

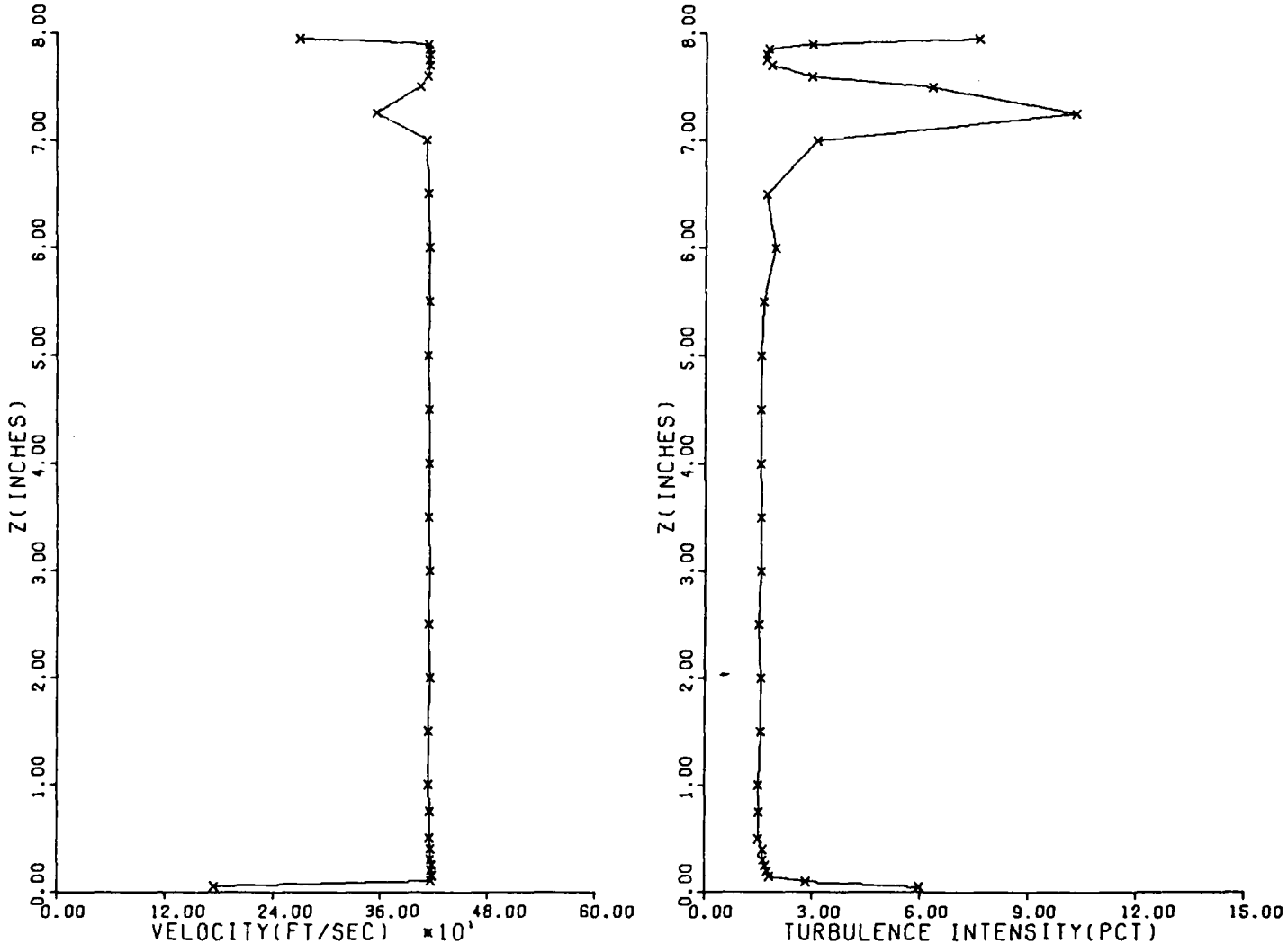

Figure 11. Velocity and Turbulence Intensity Profiles in the Stilling Chamber Exit Plane Bell Mouth Not Sealed, Y = .25 in., Exit Area = 16 Sq In.

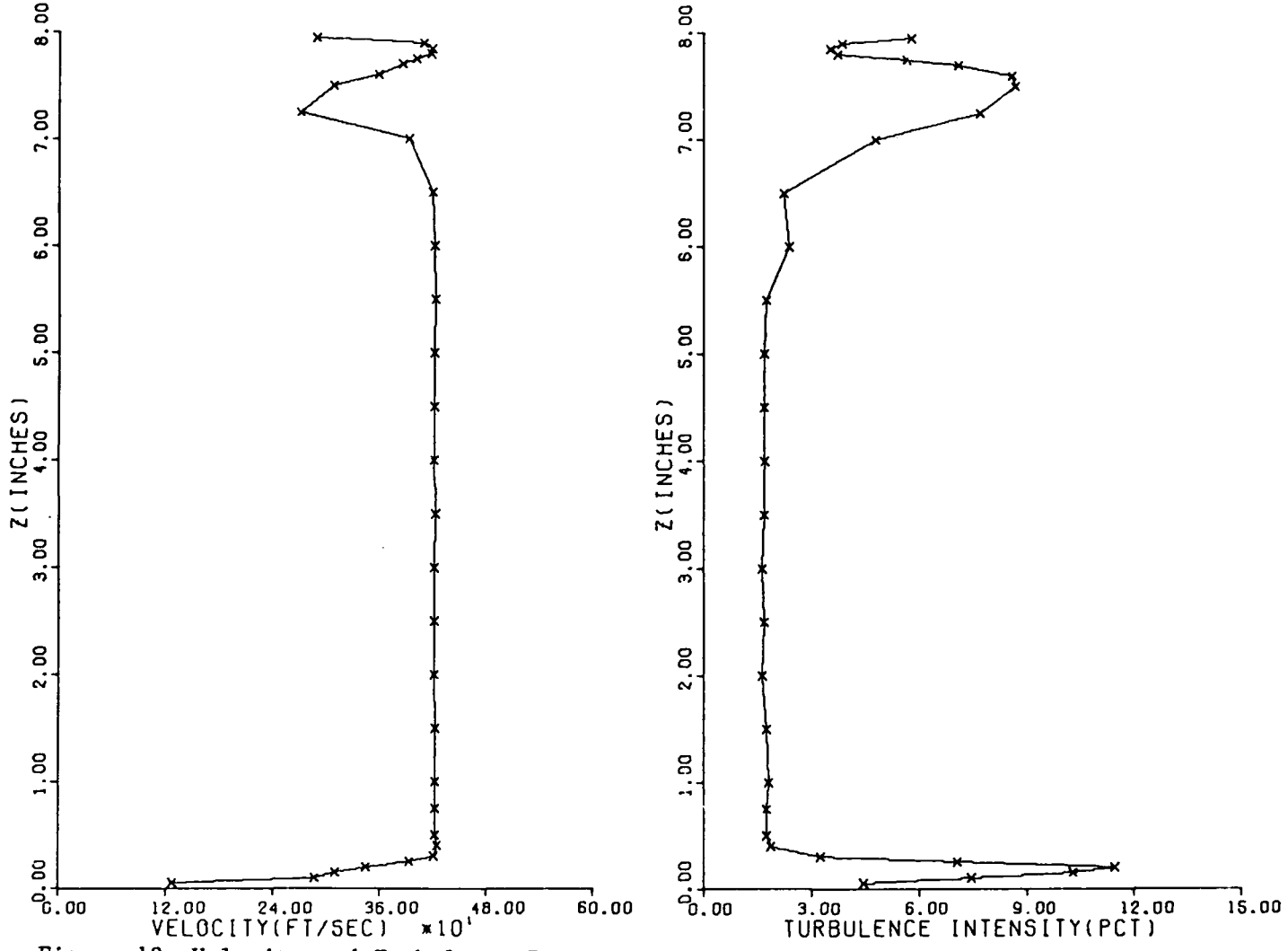

Figure 12. Velocity and Turbulence Intensity Profiles in the Stilling Chamber Exit Plane Bell Mouth Not Sealed, Y = .125 in., Exit Area = 16 sq in.

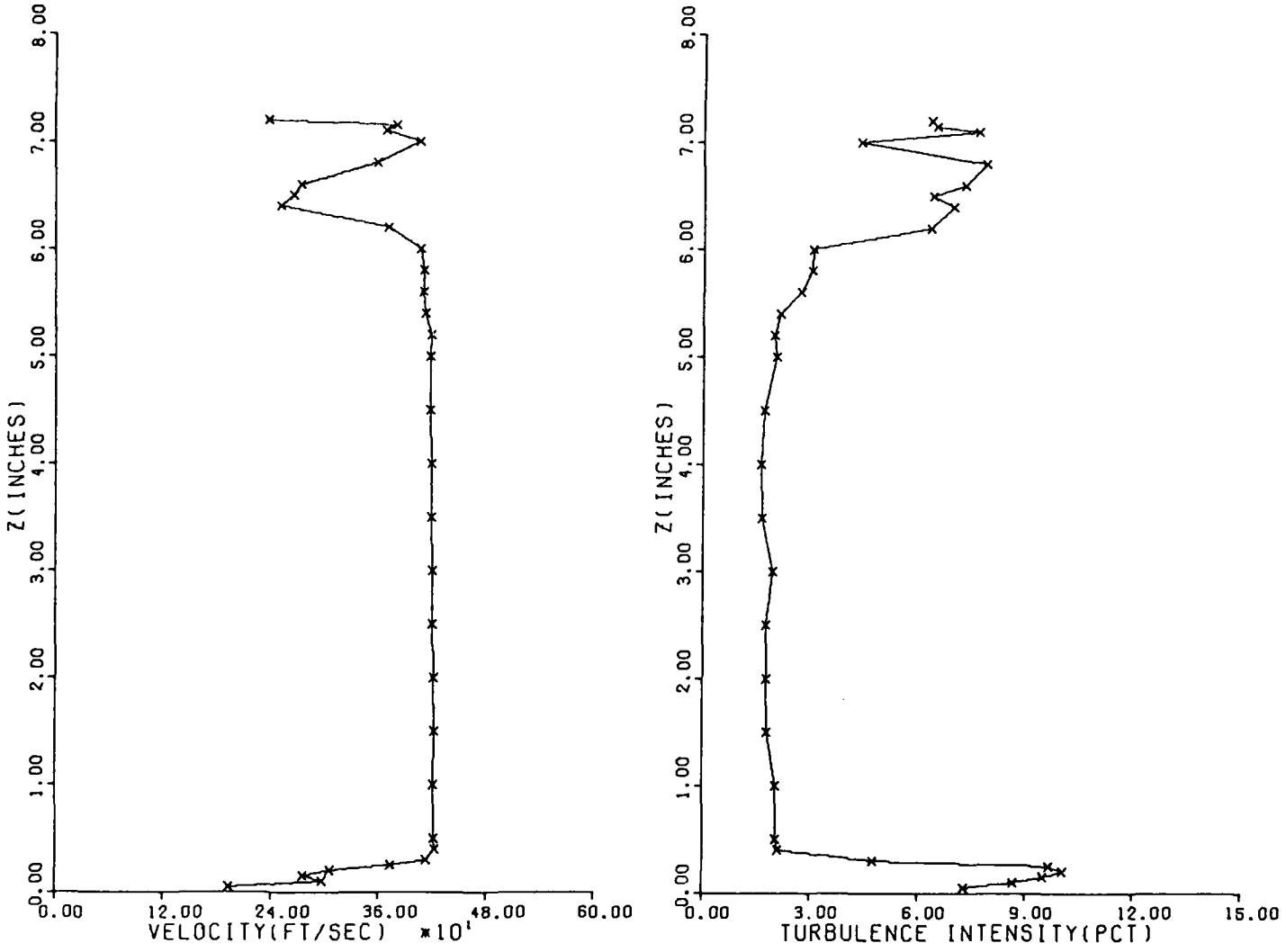

Figure 13. Velocity and Turbulence Intensity Profiles in the Stilling Chamber Exit Plane Bell Mouth Not Sealed, Y = .125 in., Exit Area = 14.5 sq in.

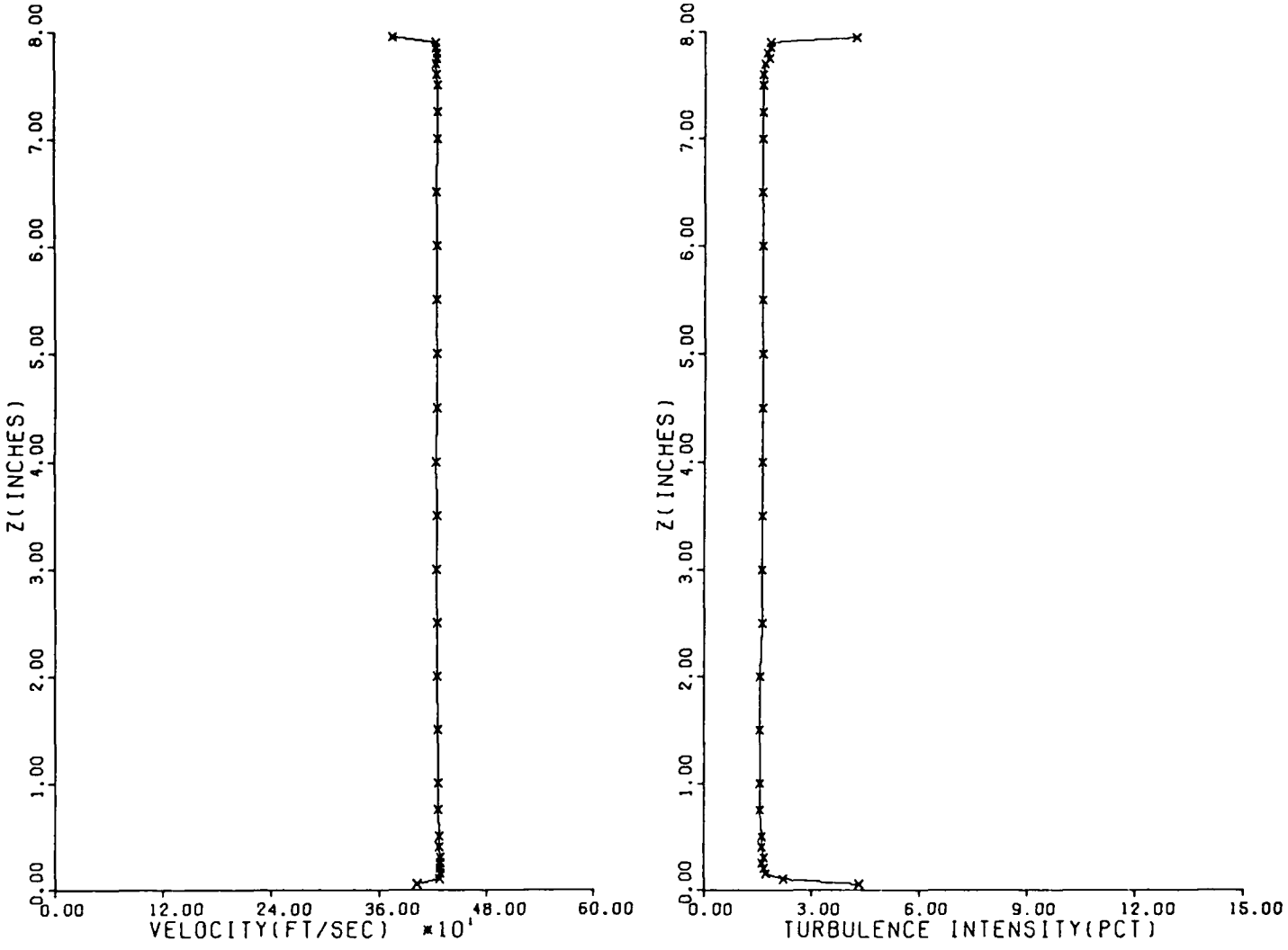

Figure 14. Velocity and Turbulence Intensity Profiles in the Stilling Chamber Exit Plane Vertical Traverse, Bell Mouth Sealed, Y = .5 in., Exit Area = 16 sq in.

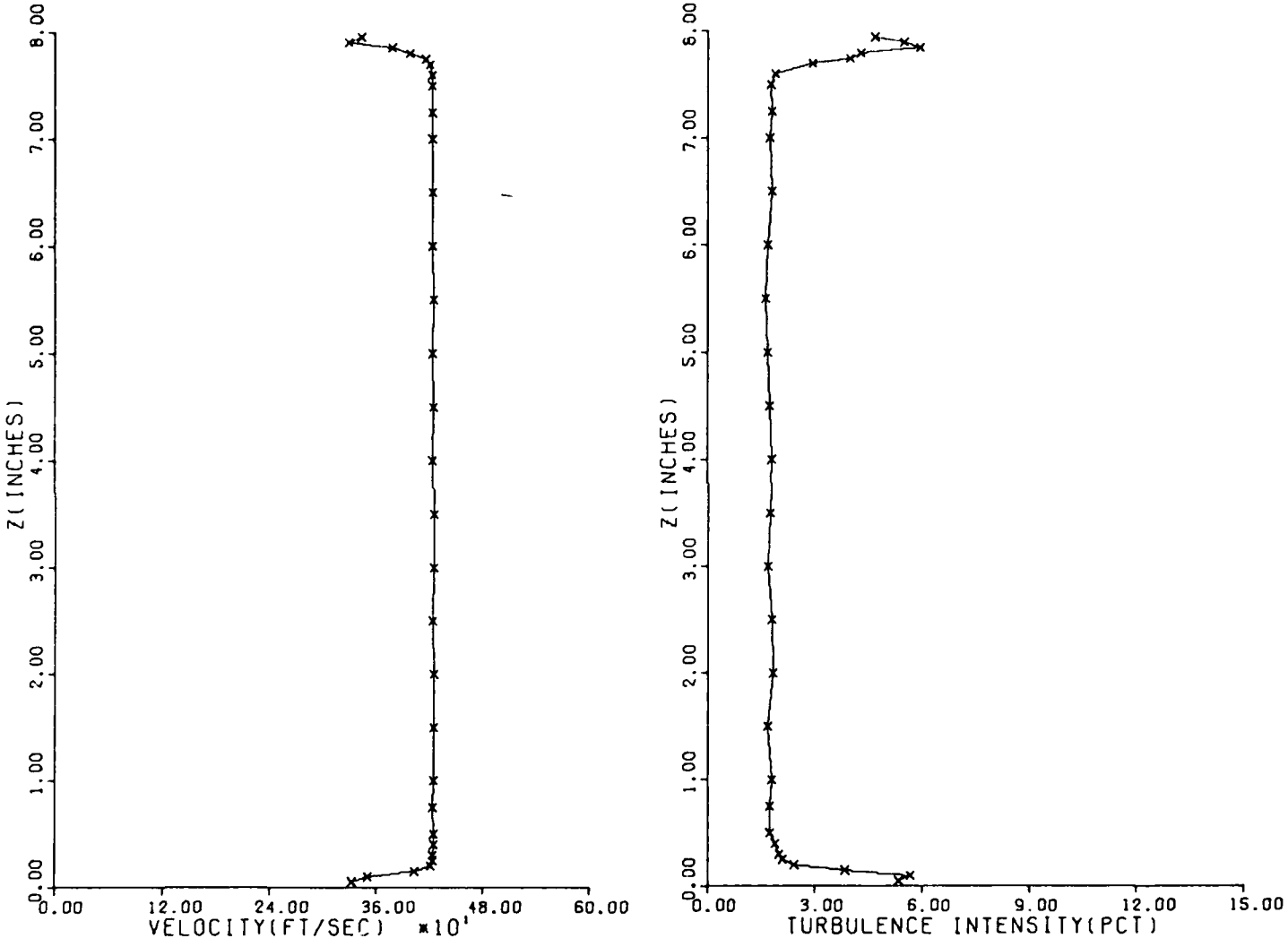

Figure 15. Velocity and Turbulence Intensity Profiles in the Stilling Chamber Exit Plane Vertical Traverse, Bell Mouth Sealed, Y = .0625 in., Exit Area = 16 sq in.

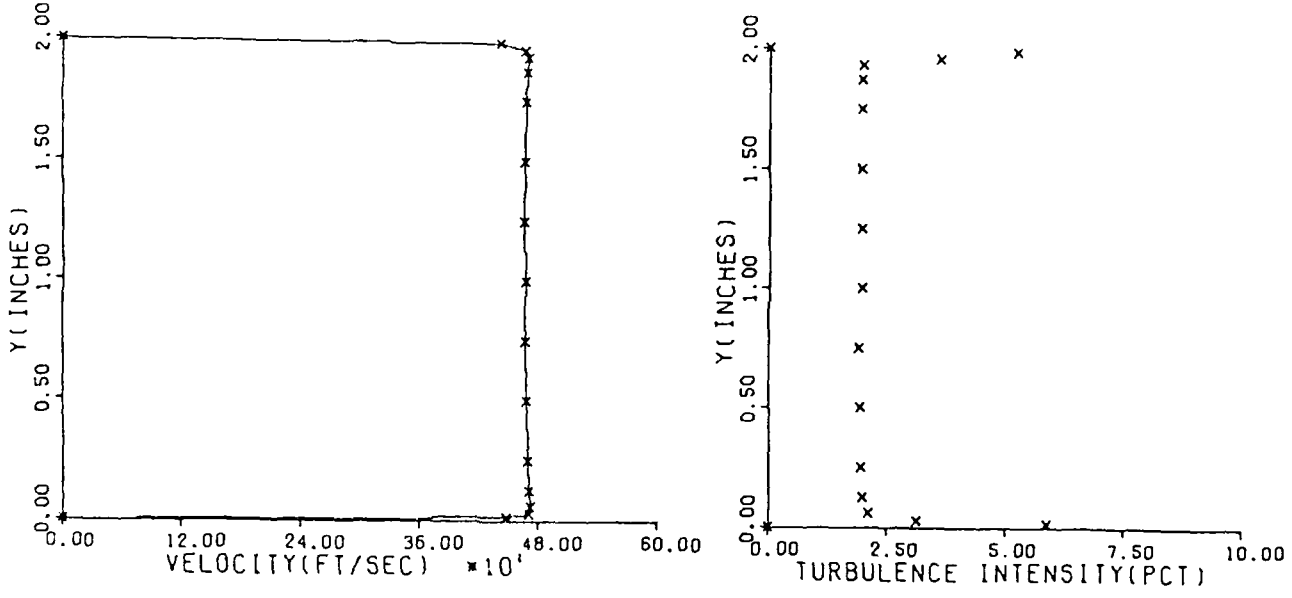

Figure 16. Velocity and Turbulence Intensity Profiles in the Stilling Chamber Exit Plane Horizontal Traverse, Bell Mouth Sealed, Z = 4.0 in.

The exit plane survey was concluded by setting the bell mouth opening at 6.86 in. in preparation for test section installation. Velocities were then calculated based on the total temperature (T_t) and pressure (P_t) in the stilling chamber and the exit plane static pressure (P). Isentropic flow through the bell mouth was assumed, and the isentropic compressible flow equations were used to find the exit plane static temperature (T)

$$T = T_t(P/P_t)^{.286} \tag{3}$$

for a specific heat ratio of 1.4. This temperature was used to find the velocity by

$$V = \sqrt{2\left(\frac{\gamma}{\gamma-1}\right)Rg(T_t-T)} \tag{4}$$

The Reynolds number was then calculated:

$$Re = \frac{\rho V l}{\mu} \tag{5}$$

with $\mu = 4.05 \times 10^{6}$ lb-sec/ft^2 (Ref. 10:67). Mass flow rates were established by

$$\dot{m} = \rho A V \tag{6}$$

with A = 13.7 sq in., the area of the opening. This area is actually too large due to boundary layer buildup along the walls, but the velocity profiles indicate that the boundary layer is very thin at the exit plane; no attempt was made to correct for the effect. Velocity, Reynolds

number, and mass flow rates are presented in Figs. 17, 18, and 19. Note that the design Reynolds number is achieved for ejector pressures greater than 50 psig.

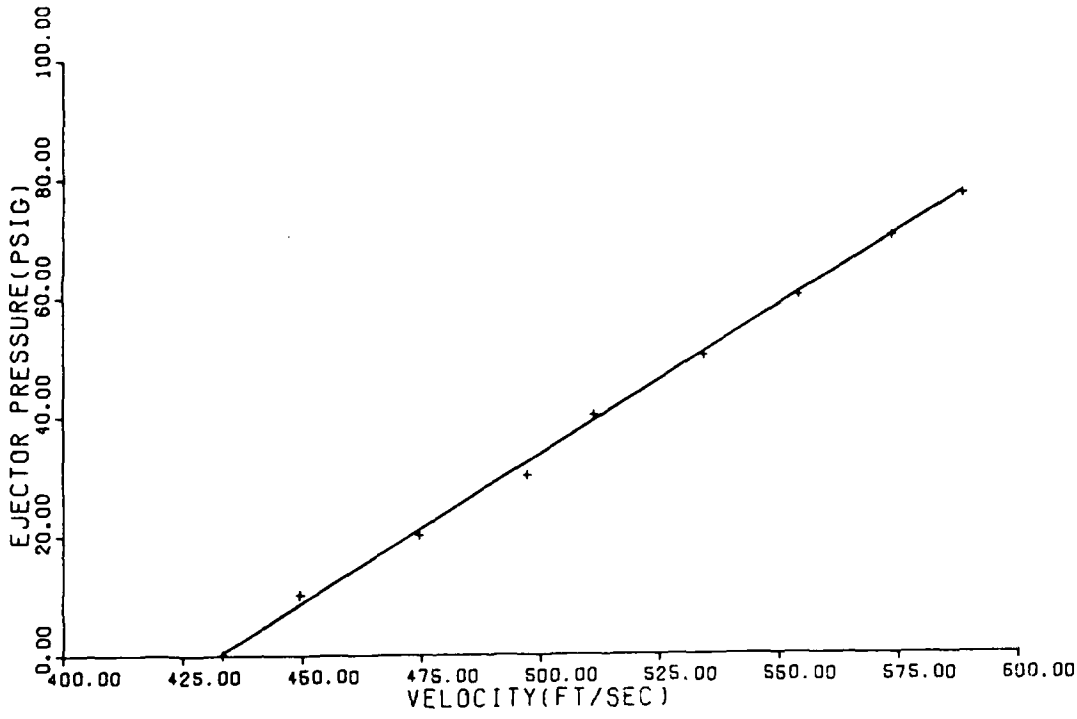

Figure 17. Stilling Chamber Exit Plane Velocity as a Function of Ejector Pressure for Exit Area = 13.7 Sq In.

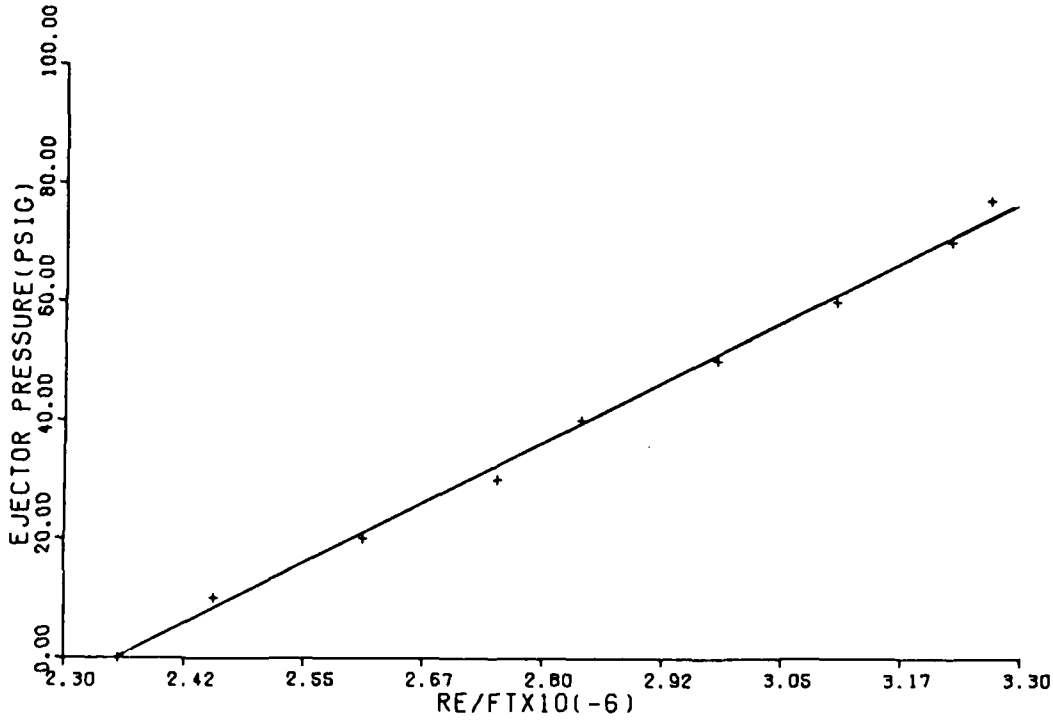

Figure 18. Stilling Chamber Exit Reynolds Number as a Function of Ejector Pressure for Exit Area = 13.7 Sq In.

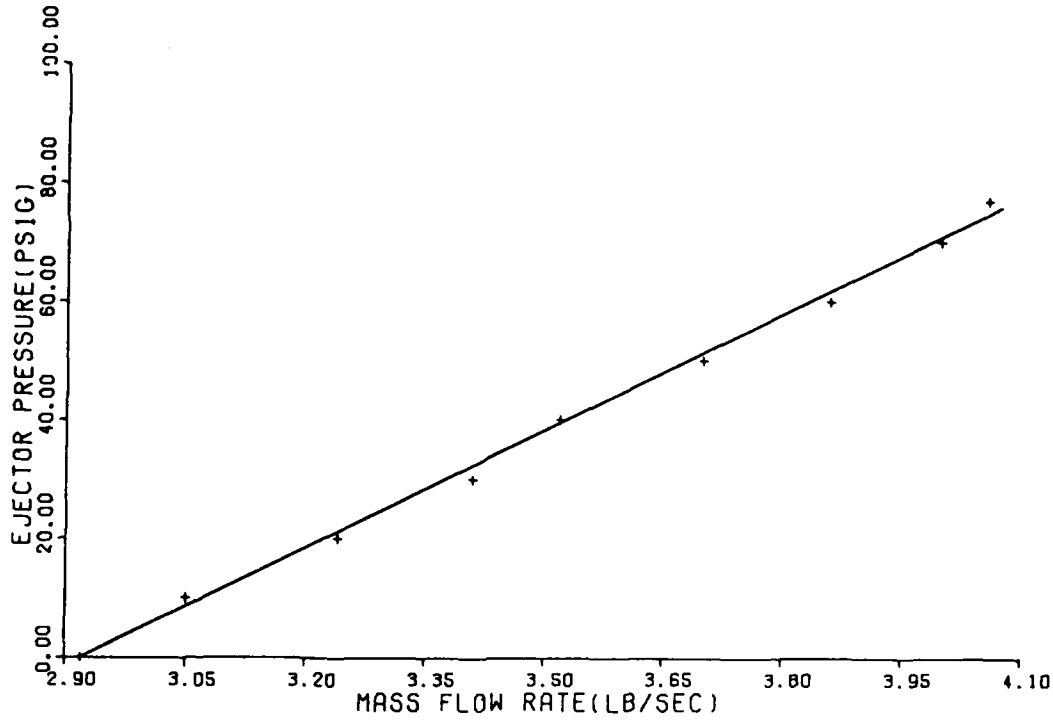

Figure 19. Facility Mass Flow Rates
for Exit Area = 13.7 Sq In.

Test Section Wake Survey

The next phase of the evaluation required the determination of the flow characteristics downstream of the cascade. Hot film anemometry measurements of velocity and turbulence intensity were made at 1 in., 4 in., and 8 in. behind the blade trailing edges at ejector pressures of 0, 40, and 50 psig. These pressures corresponded to Reynolds numbers of 2.34, 2.83, and 2.97 million per foot respectively. A summary of these results is included in Appendix B.

Figure 20 shows the wake velocity profile 1 in. behind the trailing edge at 0 psig ejector pressure. Blade number 1 is located at z = 1.3 in., as indicated by the marks on the right side of the z-axis.

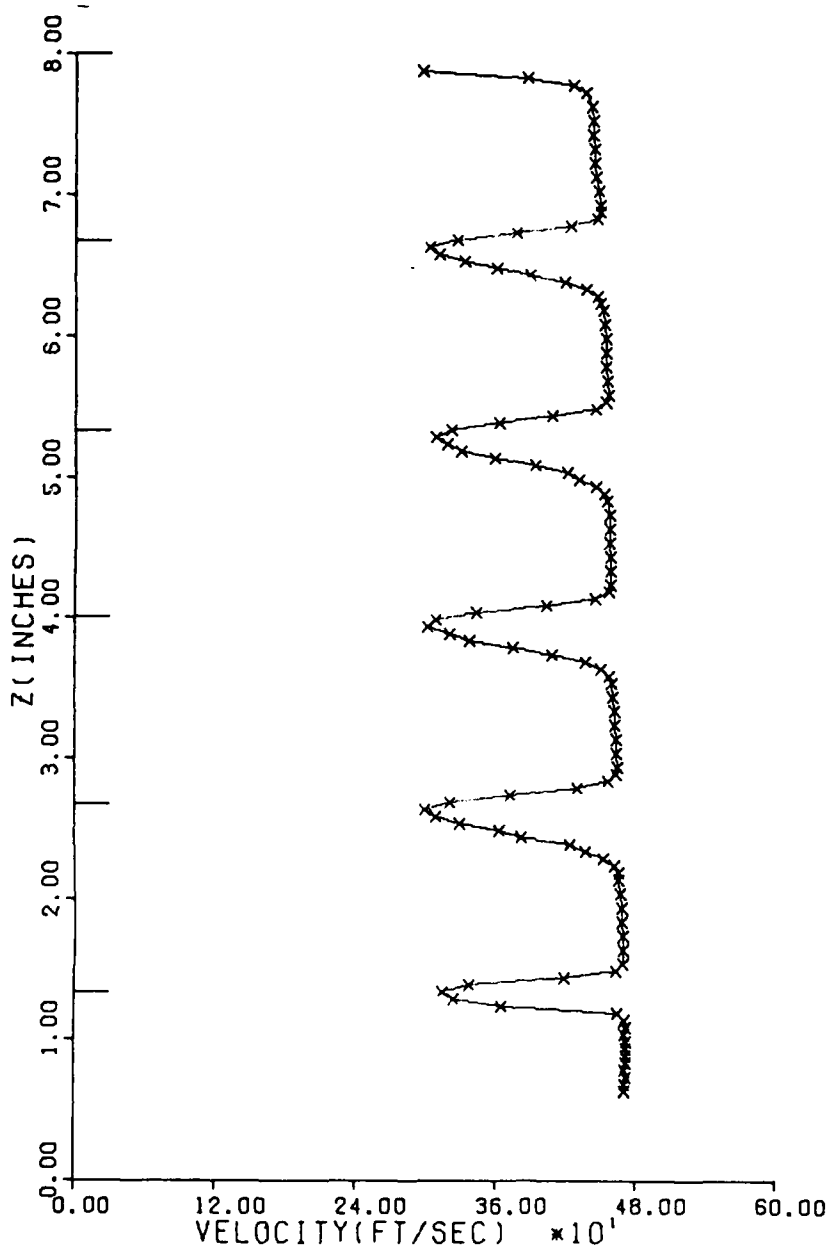

Figure 20. Wake Velocity Profile, x = 1 in., PE = 0 psig

Several characteristic features of the profile should be noted. Most important is the uniformity of the individual wake profiles. The wakes of the three center blades are virtually identical. This indicates that the five blade cascade is closely approximating an infinite cascade,

which was a major design objective. As a result of this uniformity, traverses in later studies can be made across the center blade (rather than the entire cascade) with good assurance that the data are representative of any blade in an infinite cascade.

A close examination of Fig. 20 reveals another feature of interest: the velocities outside the wakes are not constant across the test section. The exit plane survey showed that the flow field was uniform upon entrance to the test section, so the variation must be caused by the test section. The non-uniform velocity is believed to be a result of either cascade geometry or a missetting of the test section end walls. It should be noted that this velocity variation was only present in the data taken 1 in. behind the trailing edge; four inches (2 chord lengths) downstream it has damped out.

Figure 21 is a plot of turbulence intensity which corresponds to Fig. 20. The individual wake profiles are again very similar to each other. They each show a discontinuity in the profile which indicates the location of the blade trailing edge. The flow over the suction side is considerably more turbulent than that on the pressure surface, on the order of 15 to 20 percent. This is to be expected for an airfoil at high angles of attack, as the suction side flow is negotiating a severe adverse pressure gradient. Whether or not the flow has actually separated cannot be conclusively determined; however, data taken at this location would show a broad wake if the flow were separated. Furthermore, the z direction width of the "notch" in the profiles is very close to the trailing edge thickness, and the turbulence intensity decreases in a well behaved manner from the suction side maximum to the local minimum at the trailing edge. There are no random fluctuations as might

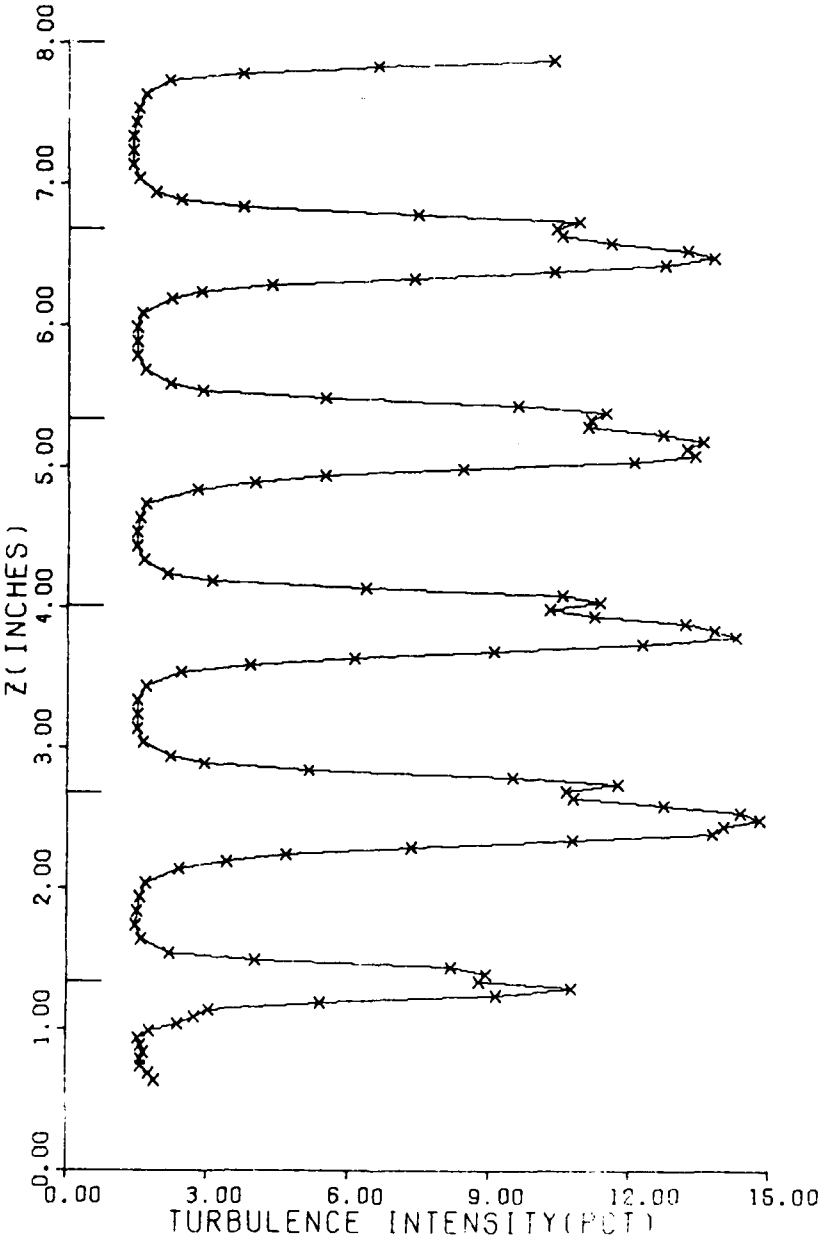

Figure 21. Wake Turbulence Intensity Profile
x = 1 in., PE = 0 psig

be expected in separated flow. A stall would also be accompanied by large deviation angles caused by the inability of the fluid to negotiate the turn; in such a case the flow would tend to migrate toward the lower end wall, resulting in higher velocities there. Profiles taken at 4 and

8 in. downstream do not show such a trend. The thicker suction side wake is explained by earlier transition to turbulent flow there than on the pressure side (Ref. 5:773). Therefore, while this evidence is not conclusive, it reinforces the hypothesis that the flow is not separated.

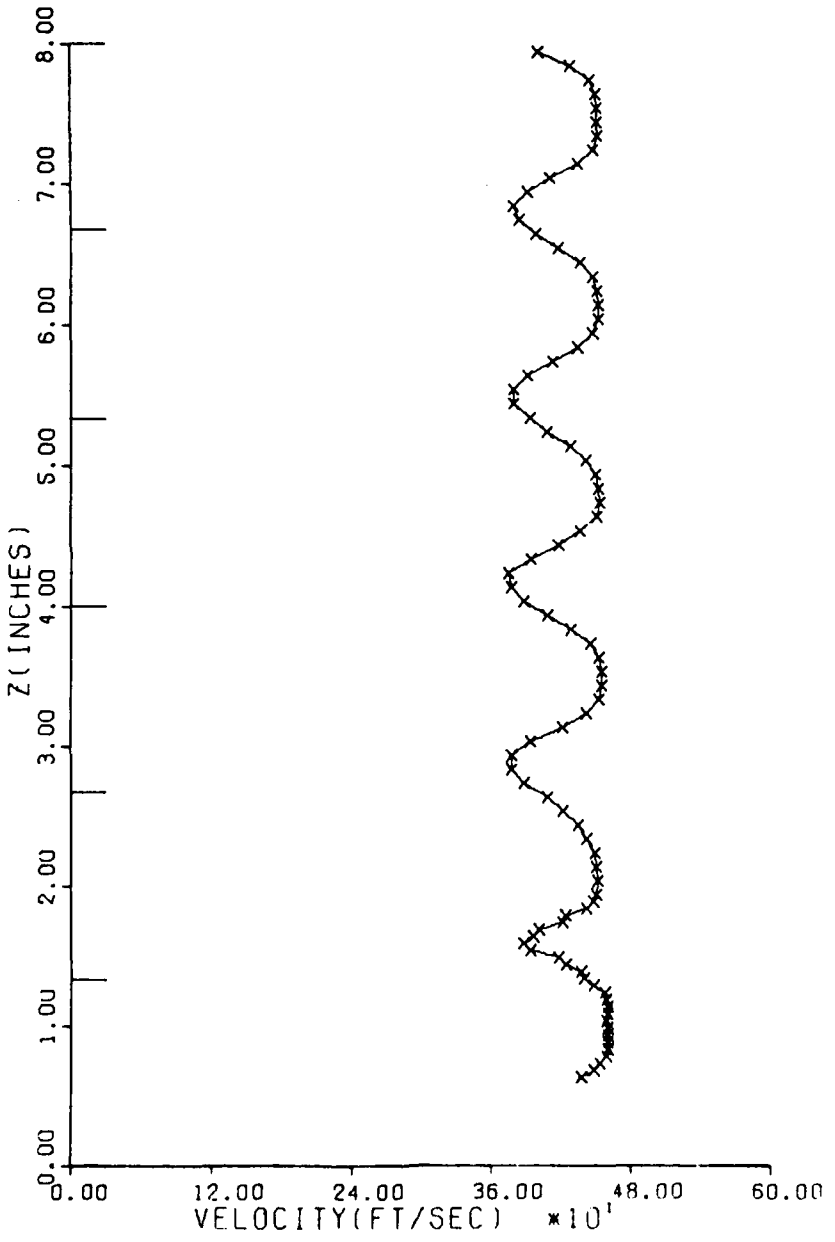

Figure 22. Wake Velocity Profile
x = 4 in., PE = 0 psig

Figure 22 shows the velocity profile 4 in. behind the trailing edge. The most notable feature of this profile is that the velocity deficit has been reduced by 50 percent from the deficit at 1 in. The wake has increased in thickness due to the momentum transfer between the wake and the undisturbed flow. This energy transfer is apparent in the corresponding turbulence intensity profile, Fig. 23.

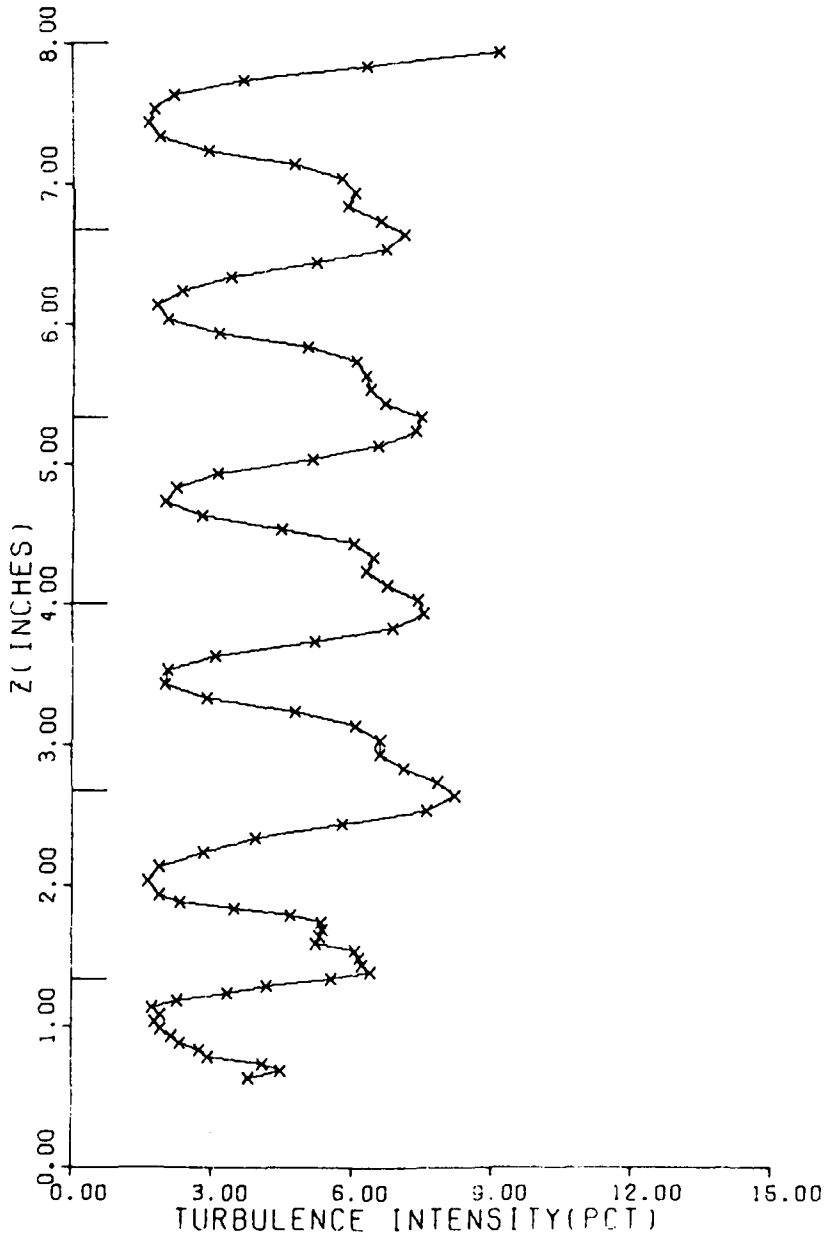

Figure 23. Wake Turbulence Intensity Profile
x = 4 in., PE = 0 psig

The profile is short and squat compared to the 1 in. profile, indicating a redistribution of the energy in the wake. Note that the minimum values of turbulence intensity are roughly 1.5 percent, nearly the same as the values at 1 in., but there is no broad area of low turbulence as before. Thus the confluence of adjacent wakes occurs approximately 4 in. behind the trailing edges.

Another notable feature of Fig. 22 is the z direction displacement of the minimum velocity point. This displacement is even more evident in the velocity profile 8 in. downstream, Fig. 24. In this plot, it is apparent that the entire wake profile has migrated in the positive z direction. Evidently the flow is not leaving the blades axially, as was the intent of the design. While this may be due to imprecise mounting of the blades, it is more likely a result of an improper adjustment of the flexible end walls (Ref. 6). This would account for the presence of a displacement despite the fact that no z direction velocity component was present 1 in. behind the trailing edge. The effect is less noticeable at higher flow velocities, as shown in Fig. 25, which is the velocity plot at the same location for an ejector pressure of 50 psig (Re = 2.97 X 10^6 per foot).

The effect of increased ejector pressure on the performance of the cascade is primarily reflected in increased flow velocity (and therefore Reynolds number). Except for the effects discussed previously, the profiles are very similar regardless of ejector pressure. The turbulence intensity plots are nearly identical for corresponding traverses, this data will not be discussed in detail. The plots are included in Appendix B.

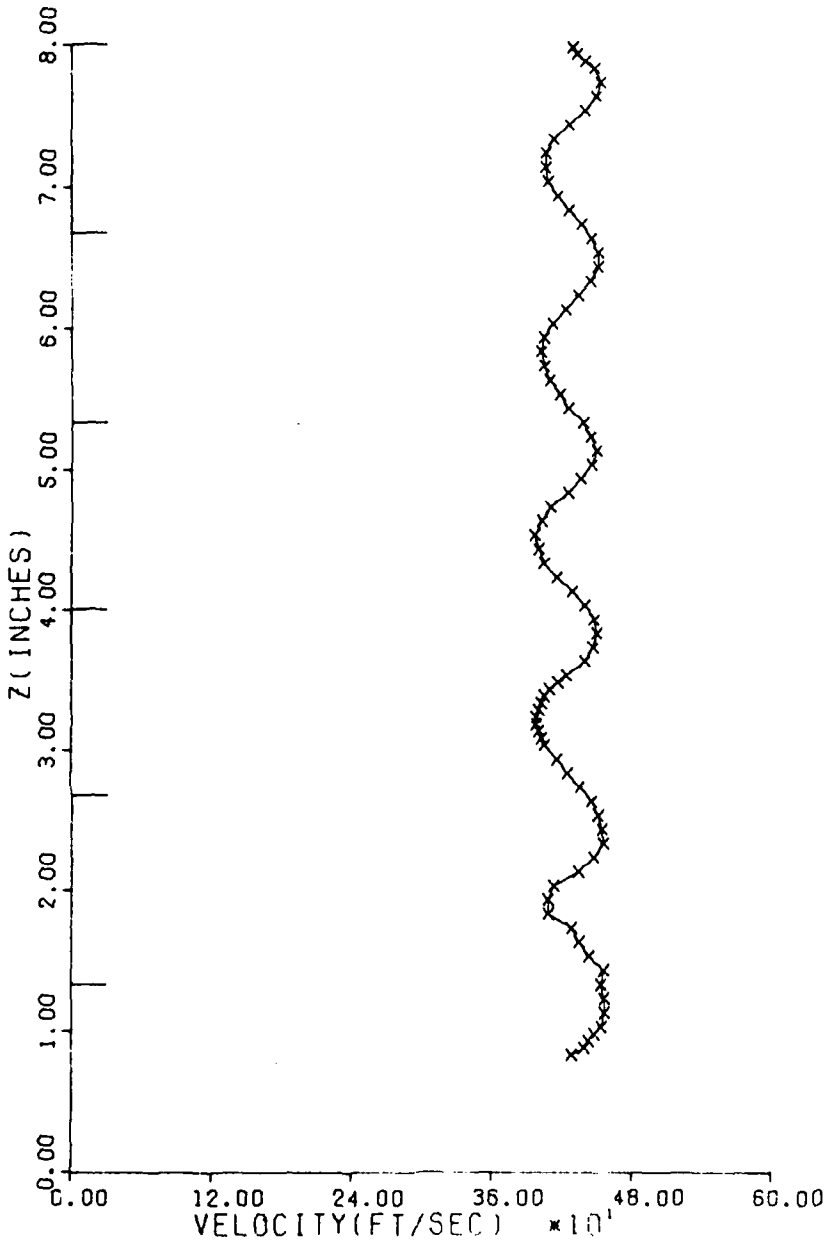

Figure 24. Wake Velocity Profile
x = 8 in., PE = 0 psig

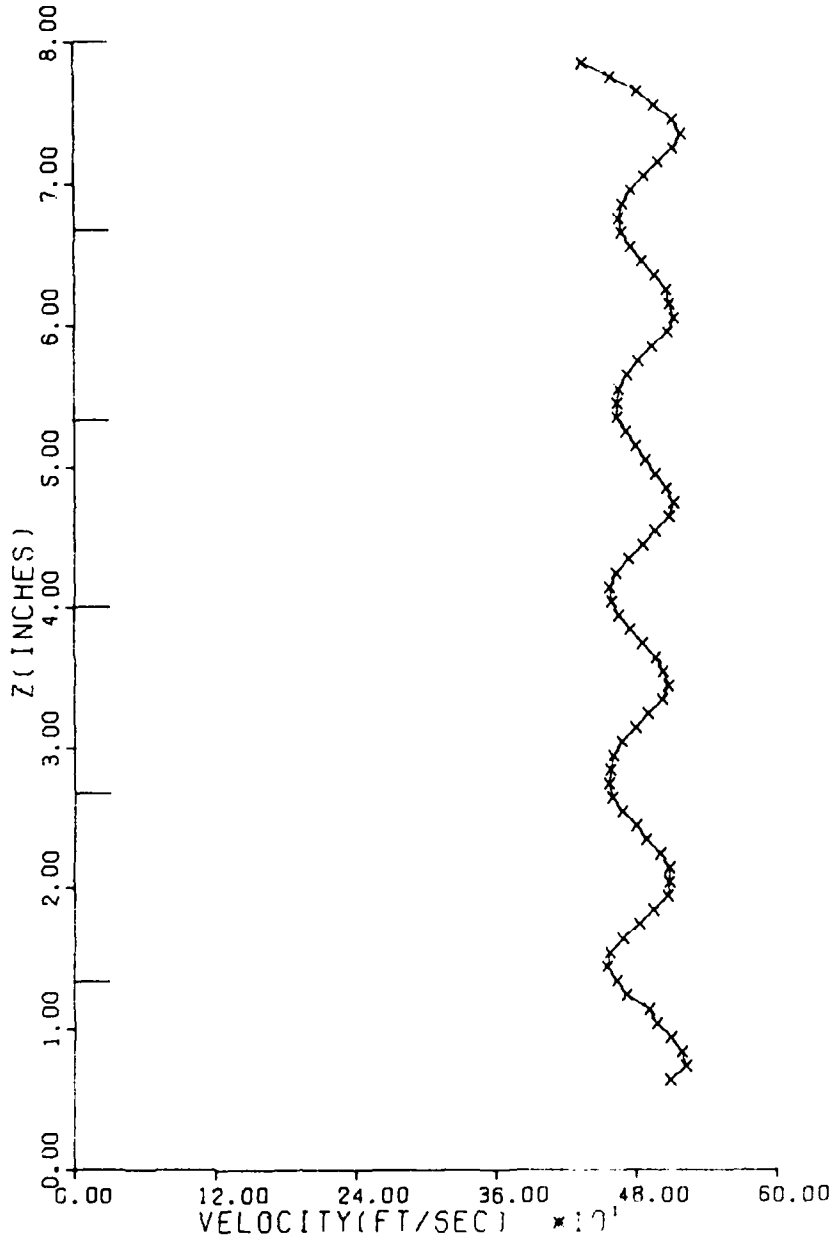

Figure 25. Wake Velocity Profile
x = 8 in., PE = 50 psig

IV. Conclusions

The evaluation tests which were described in this report indicate that the design of the Cascade Test Facility is adequate. The CTF delivers sufficient mass flow to permit testing of a cascade with a frontal area of 16 sq in. at Reynolds numbers at or above 3.0×10^6 per foot. The stilling chamber assembly allows the flow to approach the test section with turbulence intensities on the order of 2 percent. In the test section at least three blade wakes are very similar, indicating that the flow is approximating that in an infinite cascade. The instrumentation is sufficient for data collection. However, there are two items, the flexible end walls and the cascade angle of attack, which bear further investigation in order to determine their influence on the cascade flow field.

V. Recommendations

While the configuration of the CTF is satisfactory, there are several steps that could be taken to improve its usefulness. There is also one major problem area and perhaps another which need to be investigated further.

The first problem is with the flexible end walls in the test section. The position of these walls has a significant effect on the flow downstream of the cascade. The walls will have to be adjusted so that the wake does not migrate toward one of the end walls. Wall adjustment is rather difficult due to the design of the wall support, and a major redesign will probably be necessary if the walls are to be adjusted quickly and easily.

The second area of concern is the fact that the cascade may, in fact, be stalled. This could be determined by a closer investigation of the blade wakes using a multi-element sensor. The facility should also be tested using a cascade configuration known to be well below the stall in order to obtain performance profiles under these conditions.

Several minor modifications could be made to the facility which would significantly increase its utility. The first of these is the incorporation of automatic data acquisition equipment. This would allow faster data collection, which means the data for a given traverse would be obtained under more uniform conditions, while reducing the time the fragile anemometer sensors are exposed to the flow. Secondly, placing a static temperature probe on the anemometer probe would reduce experimental error, since these temperatures can only be estimated with the

present instrumentation. This inaccuracy affects the Reynolds number calculation in both the density and viscosity terms. Thirdly, a better arrangement for controlling the ejector pressure is needed. The system is quite sensitive and increases run time because frequent adjustments are necesary to maintain the proper pressure. Fourth, an electronic air cleaner should be installed in the stilling chamber; sensor destruction due to dust impingement was a major problem, and will be even worse if smaller, more sensitive sensors are used. Fifth, the bell mouth should be modified to incorporate an integral seal. This will be particularly important if the facility is used as a wind tunnel rather than as a cascade facility. Finally, the performance of the CTF could possibly be improved by attempting to optimize the ejector performance. As stated previously, no real attempts were made at optimization, even though the ejector was designed with this flexibility in mind.

Bibliography

1. Vonada, John A. Wake Mixing Investigation of Crenelated Vane Trailing Edges (tentative title). Unpublished Ph.D. Dissertation. Wright-Patterson AFB, Ohio: Air Force Institute of Technology.

2. Genovese, David. The Effect of Surface Roughness on Blade Performance in Cascade (tentative title). Unpublished MS Thesis. Wright-Patterson AFB, Ohio: Air Force Institute of Technology.

3. Keenan, J.H., and E.P. Neumann. "A Simple Air Ejector", Journal of Applied Mechanics, 64, 1942.

4. Keenan, J.H., et al. "An Investigation of Ejector Design by Analysis and Experiment," Journal of Applied Mechanics, 17, 1950.

5. Schlichting, Hermann. Boundary Layer Theory (Seventh Edition). Translated by J. Kestin. New York: McGraw-Hill Book Company, 1979.

6. Erwin, John R., and James C. Emery. NACA TR 1016: Effect of Tunnel Configuration and Testing Technique on Blade Performance. Langley Field, Virginia: Langley Aeronautical Laboratory, November 1949.

7. Hernandez, Enrique G. An Interactive Computational Aerodynamics Analysis Program. MS Thesis. Wright-Patterson AFB, Ohio: Air Force Institute of Technology, December 1980.

8. Elrod, W.C. Lecture Materials presented in ME 7.33, Airbreathing Engine Design. School of Engineering, Air Force Institute of Technology, Wright-Patterson AFB, Ohio, April 1981.

9. Vincent, E.T. The Theory and Design of Gas Turbines and Jet Engines. New York: McGraw-Hill Book Company, 1950.

10. Dommasch, Daniel O., et al. Airplane Aerodynamics (Fourth Edition). New York: Pitman Publishing Corporation, 1967.

11. Kirchner, Michael J. Computer Assisted Velocity and Turbulence Measurements in a Plane Free Jet at High Subsonic Velocities. MS Thesis. Wright Patterson AFB, Ohio: Air Force Institute of Technology, December 1981.

12. Thermo-Systems, Incorporated. Operating and Service Manual for 1050 Series Constant Temperature Anemometers and Related Accessories, (undated).

Appendix A: Data Collection and Reduction

Data Collection

The hot wire/hot film anemometer was selected as the primary means of obtaining flow data for the CTF. The advantages of the hot wire over pitot-static systems are numerous. Primary among these advantages are the capability to measure both velocity and turbulence parameters simultaneously, and to easily interface with a computerized data collection and reduction system. Unfortunately, the sensors are very fragile and are broken easily by impinging dust particles. This represented the major drawback to the anemometry system during the study. A Thermo Systems, Incorporated (TSI) model 1050 anemometry system was used for this study, with a TSI 1214-20 single wire hot film sensor of diameter .002 in. This rather large diameter was used due to the presence of dust particles entering the CTF through the ejector air supply. While the frequency response of the large sensor decreased the accuracy of the turbulence data, the decrease was not considered to be significant within the scope of the facility evaluation. Smaller, more sensitive sensors should be used for data collection requiring high accuracy.

An accurate calibration of the hot film sensors was necessary in order to convert the voltage outputs of the anemometer into usable data. The calibrations for the sensors used in this study were performed on the AFIT Hewlett-Packard Automatic Data Acquisition System, using a procedure developed by Kirchner (Ref. 11). This procedure allows semi-automatic calibration of the probe, and provides the coefficients for

and a plot of a fourth order polynomial calibration curve.

The voltage outputs from the anemometer were fed into two voltmeters: a Digitec model 268 Direct Current (DC) voltmeter and a Hewlett-Packard model 3400A Root Mean Square (RMS) voltmeter. The DC and RMS voltages were recorded at each data point, and were converted to velocities and turbulence intensities, respectively, by a FORTRAN computer program using the Control Data Corporation 6600 computer at AFIT.

Data Reduction

The data reduction program used a polynomial evaluation routine to convert voltages to velocities. However, the voltages were first corrected for the static temperature of the flow being different from the probe calibration static temperature. This correction was necessary because the heat transfer from the sensor to the flow is quite sensitive to the ambient static temperature. Failure to correct for this effect yielded velocity inaccuracies of between 15 and 20 percent when compared to pitot-static calculations at velocities of 500-600 feet per second. With the temperature correction applied, the pitot-static and anemometer velocities agreed to within approximately 3 percent. The temperature correction factor (TCF) was calculated using the formula

$$TCF = \sqrt{\frac{(\text{Sensor Temp} - \text{Calibration Temp})}{(\text{Sensor Temp} - \text{Total Temp})}} \qquad (7)$$

where Sensor Temp is the nominal sensor operating temperature (450 F), Calibration Temp is the calibration total temperature, and Total Temp is the total temperature at a data point for a given flow condition (Ref. 12). The "raw" DC voltages were multiplied by the TCF, and then

converted to velocities using a fourth order polynomial:

$$V = a_0 + a_1 v + a_2 v^2 + a_3 v^3 + a_4 v^4 \tag{8}$$

where V is the velocity and v is the corrected voltage. The coefficients were obtained from the probe calibration described above.

The turbulence intensity was calculated by

$$TI = \frac{m v_{RMS}}{V_{max}} \tag{9}$$

where m is the slope of the calibration curve, v_{RMS} is the RMS voltage at the data point (corrected for temperature effects), and V_{max} is the maximum velocity measured during a traverse. Figure 26 shows the computation graphically.

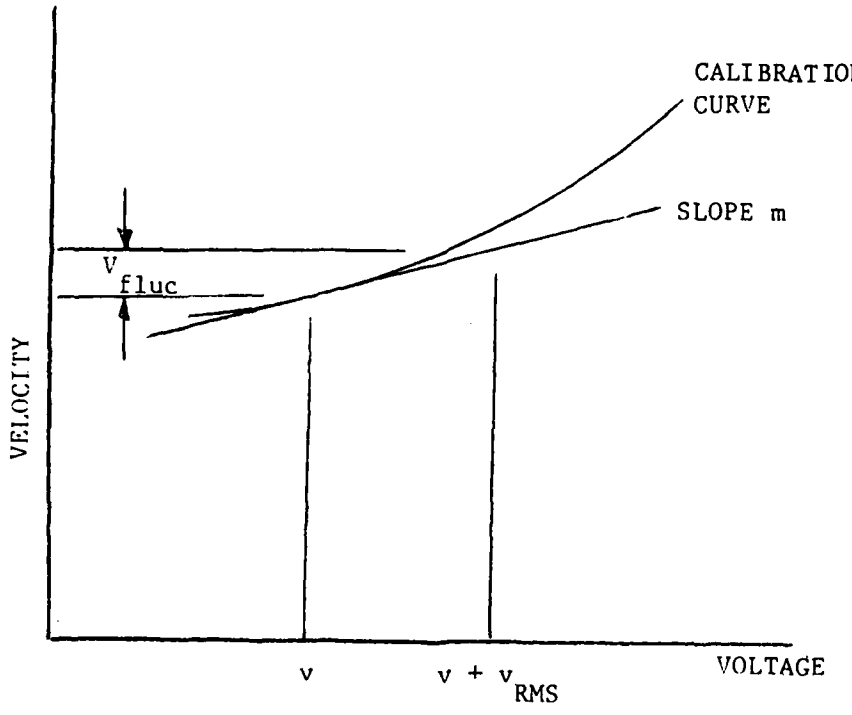

Figure 26. Fluctuating Velocity Calculation

Here, $V_{fluc} = mv_{RMS}$ and represents the fluctuating velocity. The drawing indicates that the calculated fluctuating velocity will be smaller than the actual fluctuating velocity, resulting in lower calculated turbulence intensities. However, the calibration curve is very nearly linear in this range, and the RMS voltage is small. As a result, the error introduced by using the linear approximation is negligible.

Appendix B: Wake Velocity and Turbulence Intensity Profiles

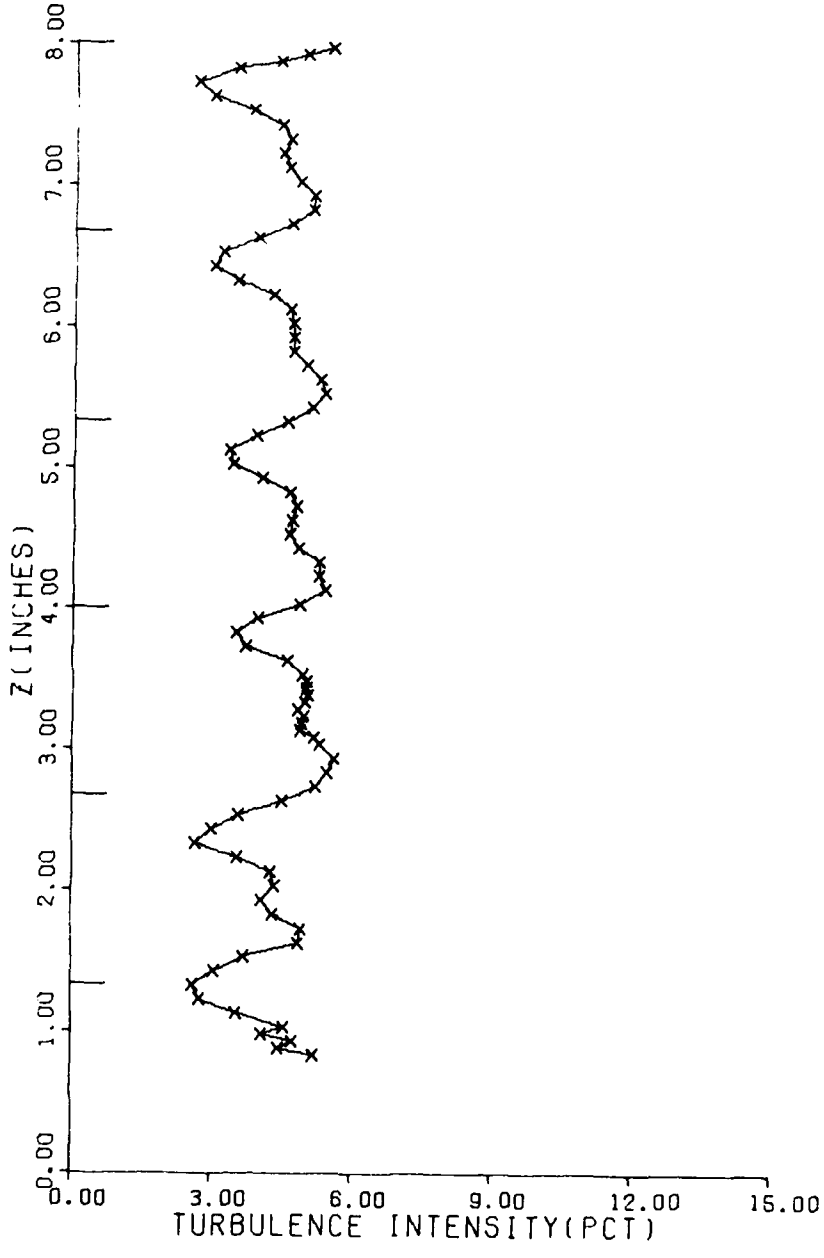

Figure 27. Wake Turbulence Intensity Profile
X = 8 in., PE = 0 psig

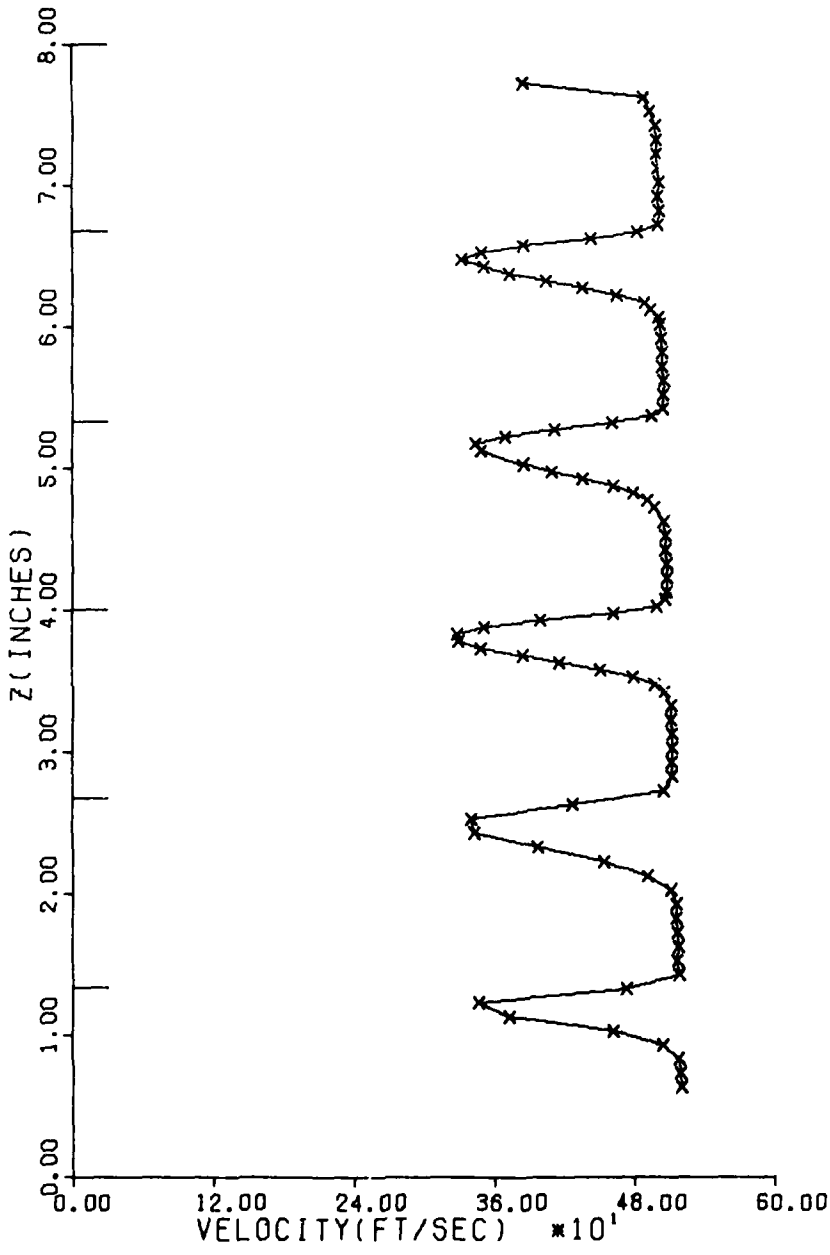

Figure 28. Wake Velocity Profile
X = 1 in., PE = 40 psig

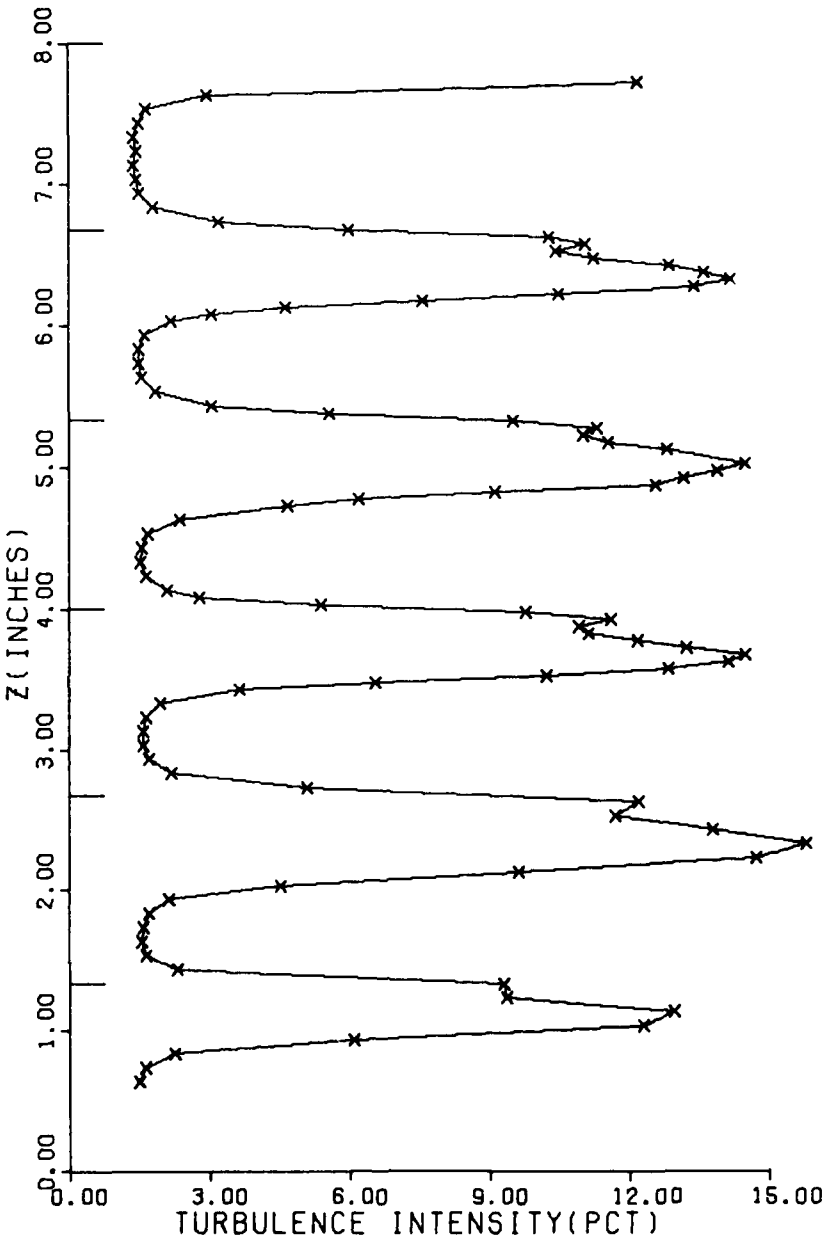

Figure 29. Wake Turbulence Intensity Profile
X = 1 in., PE = 40 psig

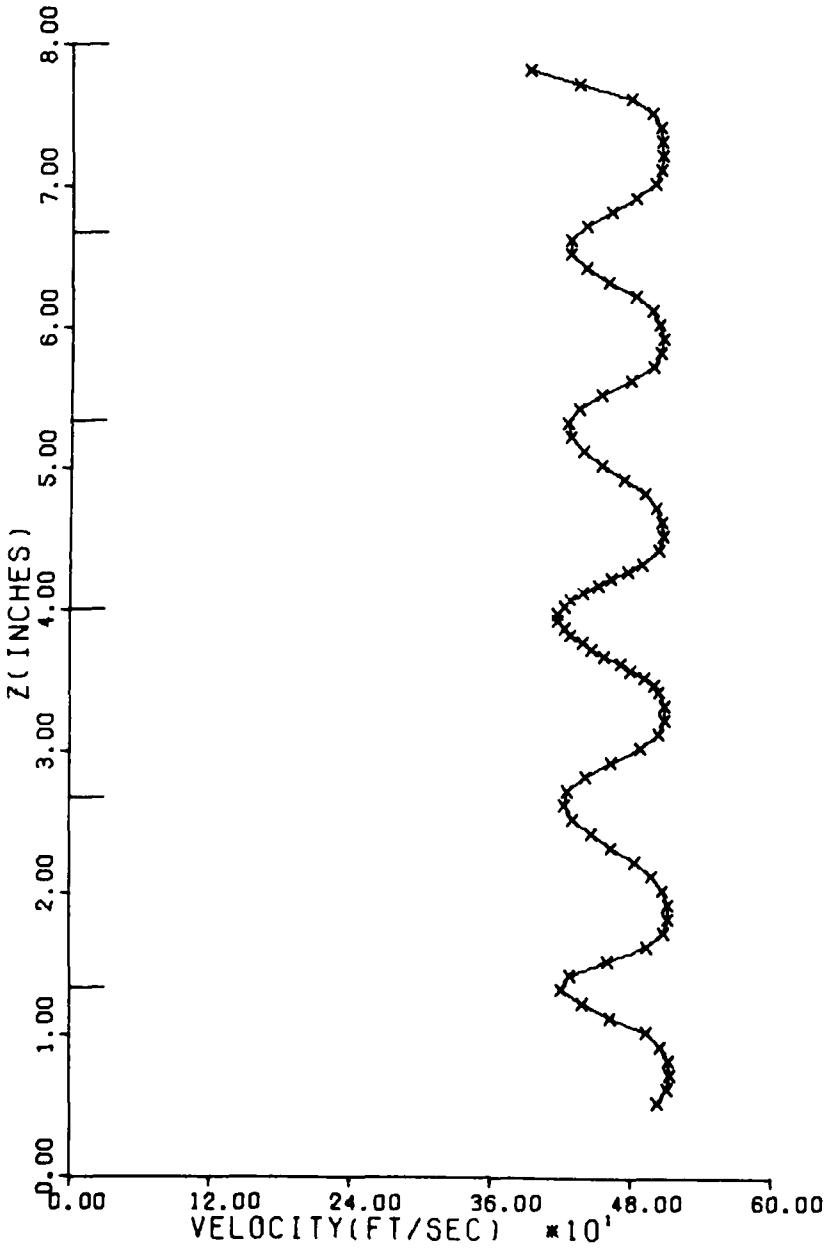

Figure 30. Wake Velocity Profile
X = 4 in., PE = 40 psig

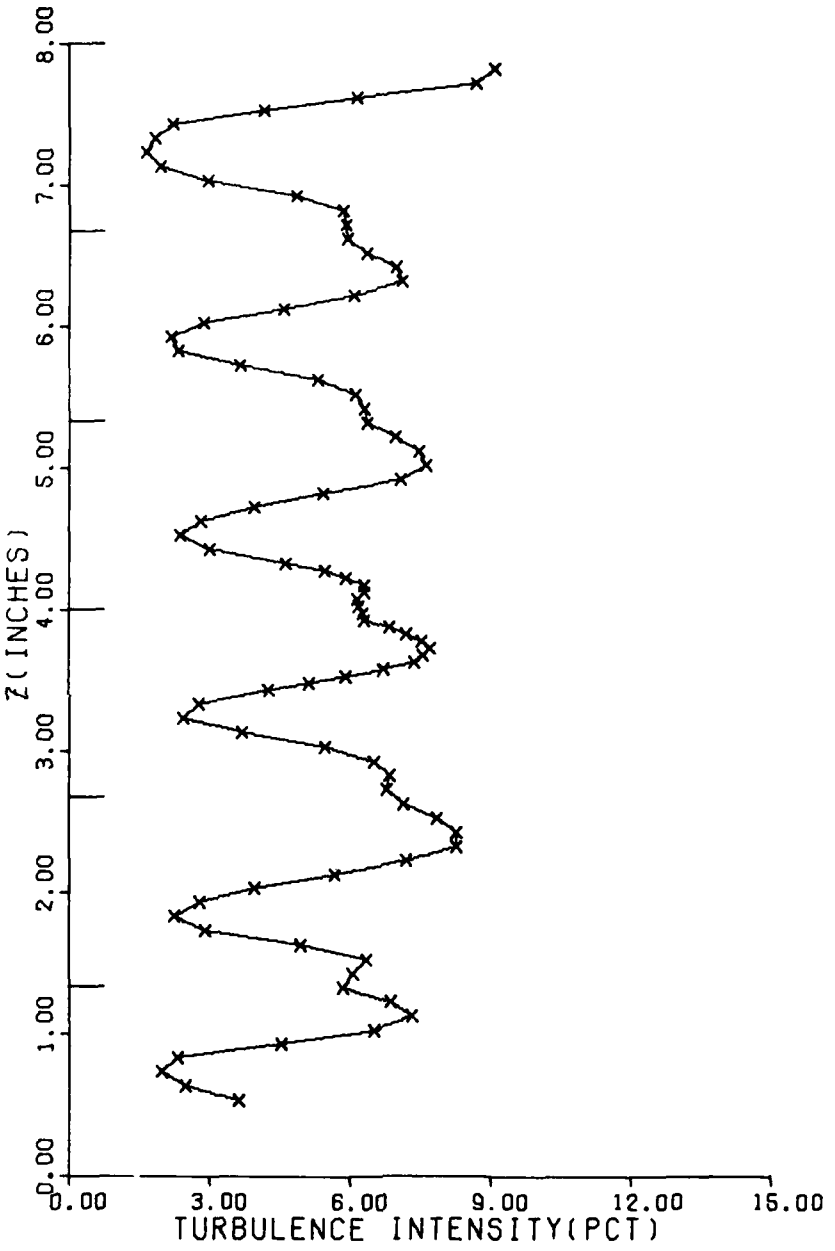

Figure 31. Wake Turbulence Intensity Profile
X = 4 in., PE = 40 psig

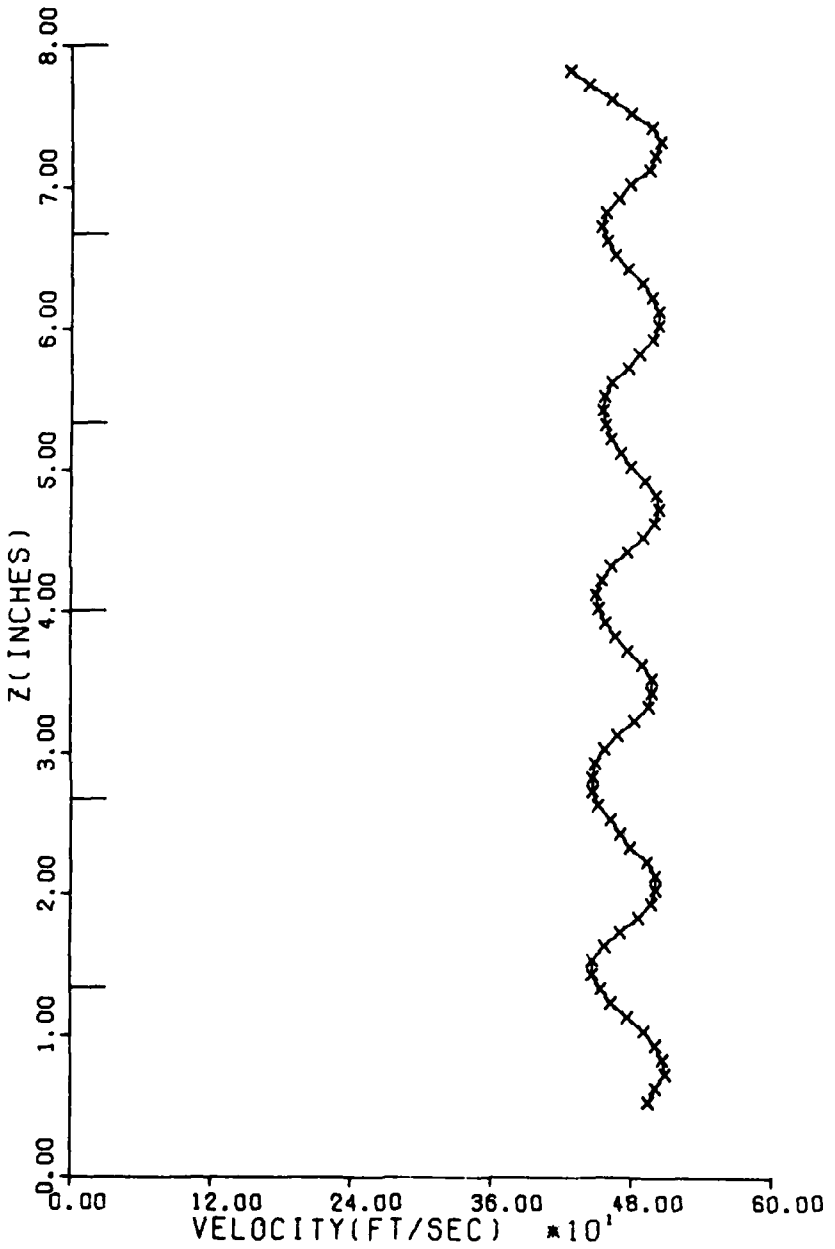

Figure 32. Wake Velocity Profile
X = 8 in., PE = 40 psig

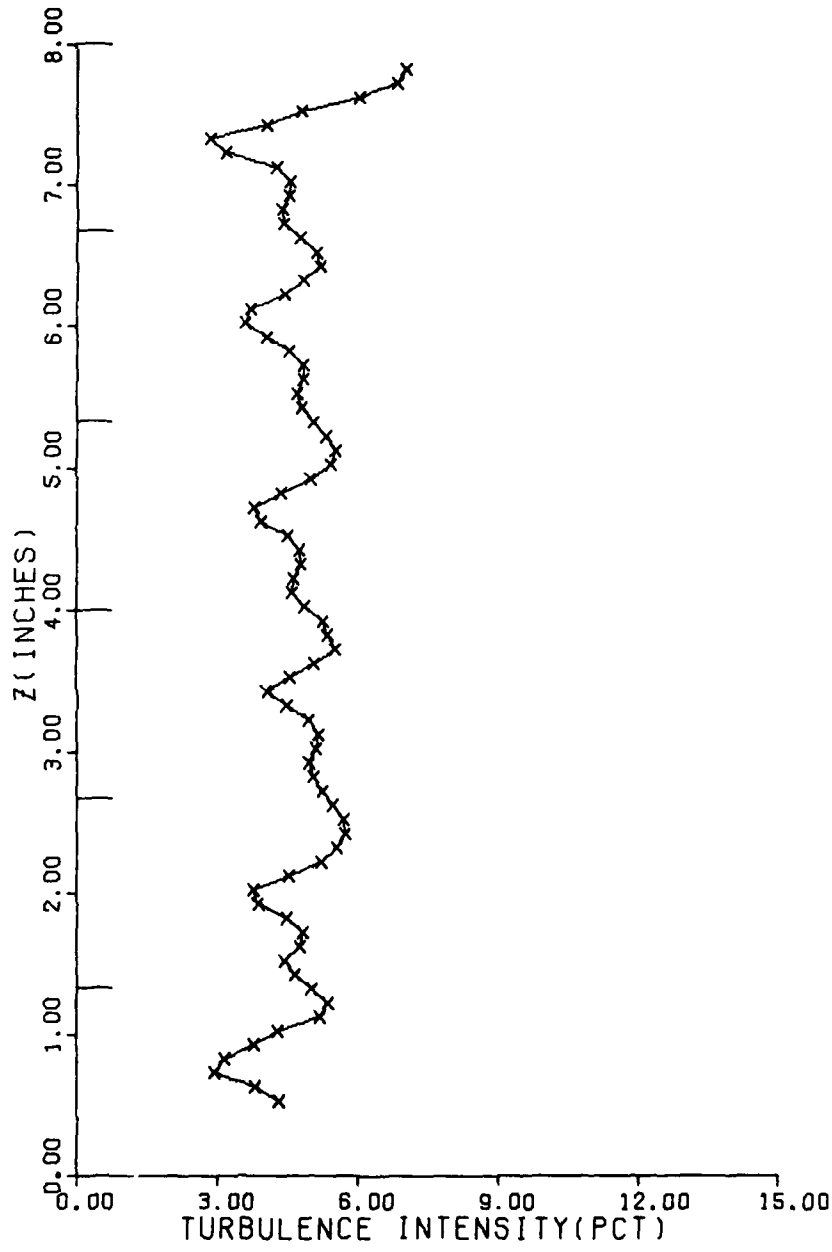

Figure 33. Wake Turbulence Intensity Profile
X = 8 in., PE = 40 psig

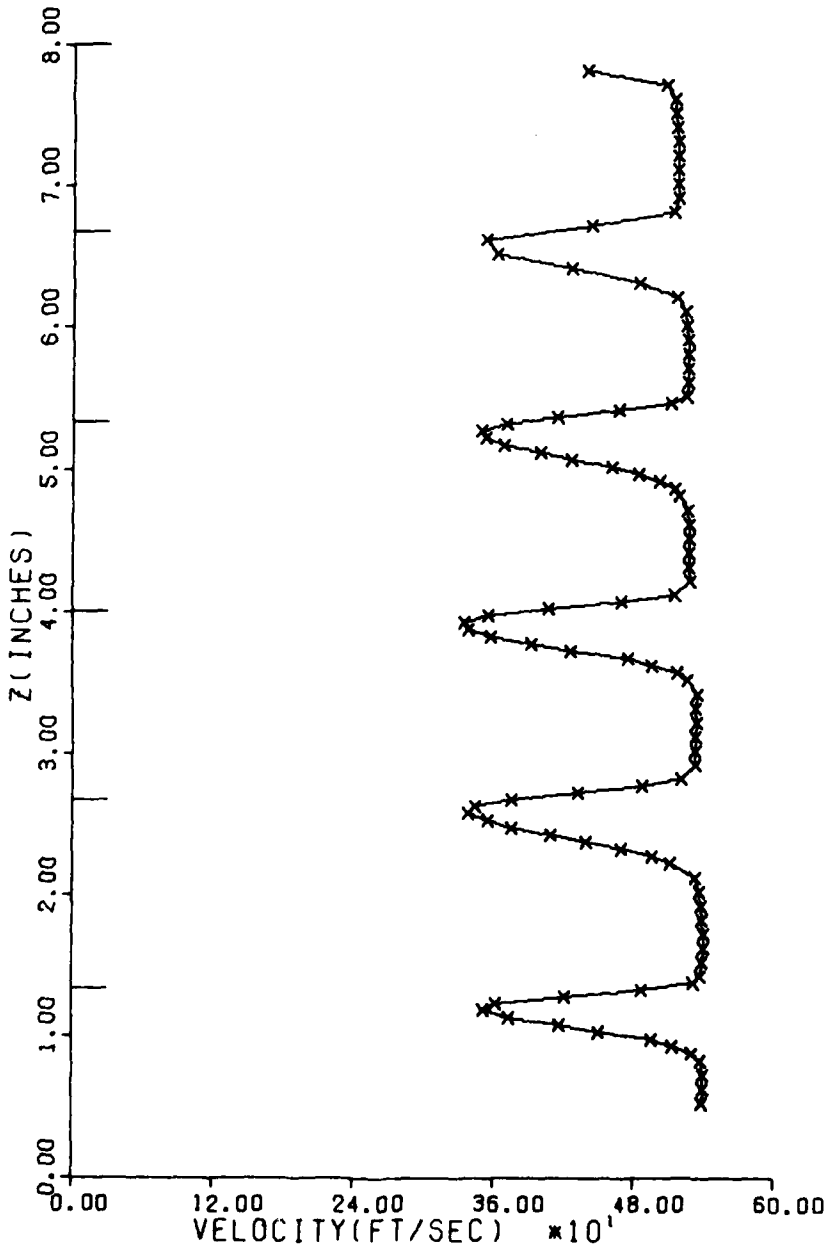

Figure 34. Wake Velocity Profile
X = 1 in., PE = 50 psig

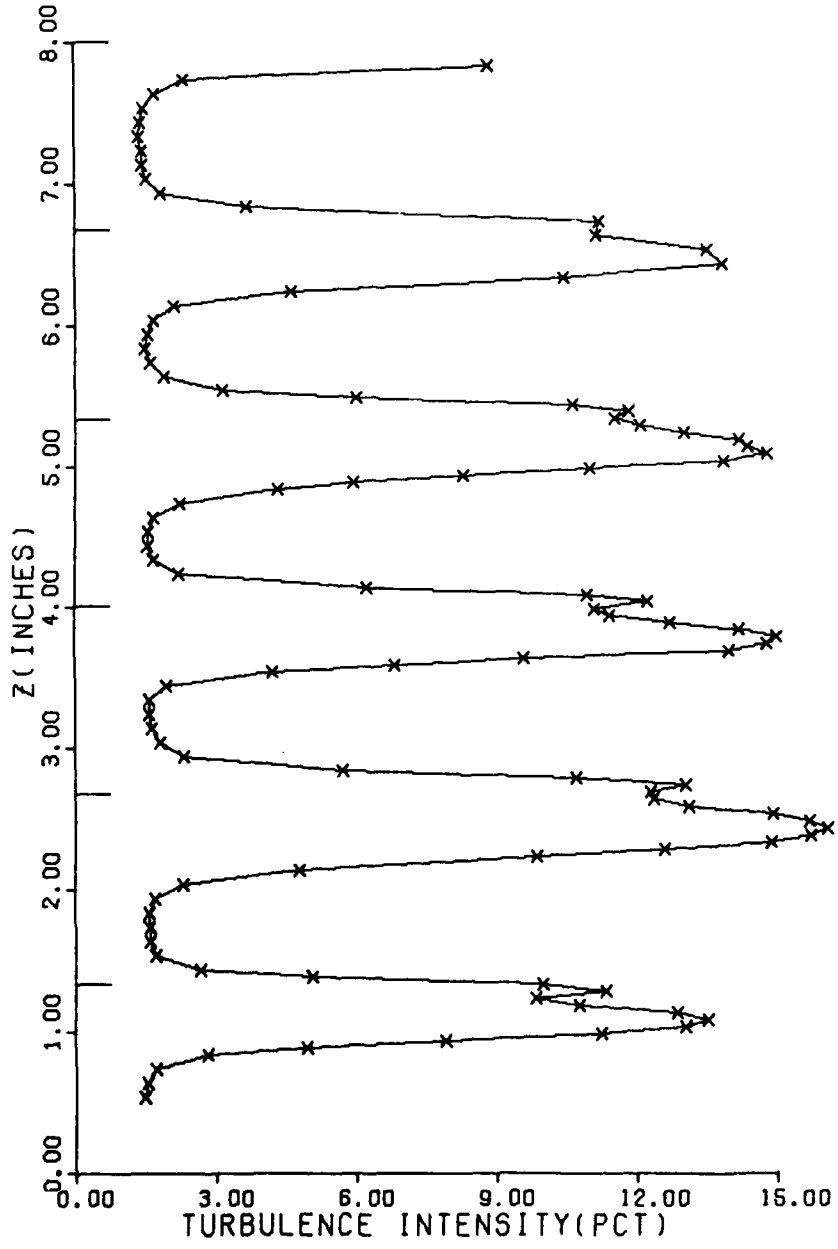

Figure 35. Wake Turbulence Intensity Profile
X = 1 in., PE = 50 psig

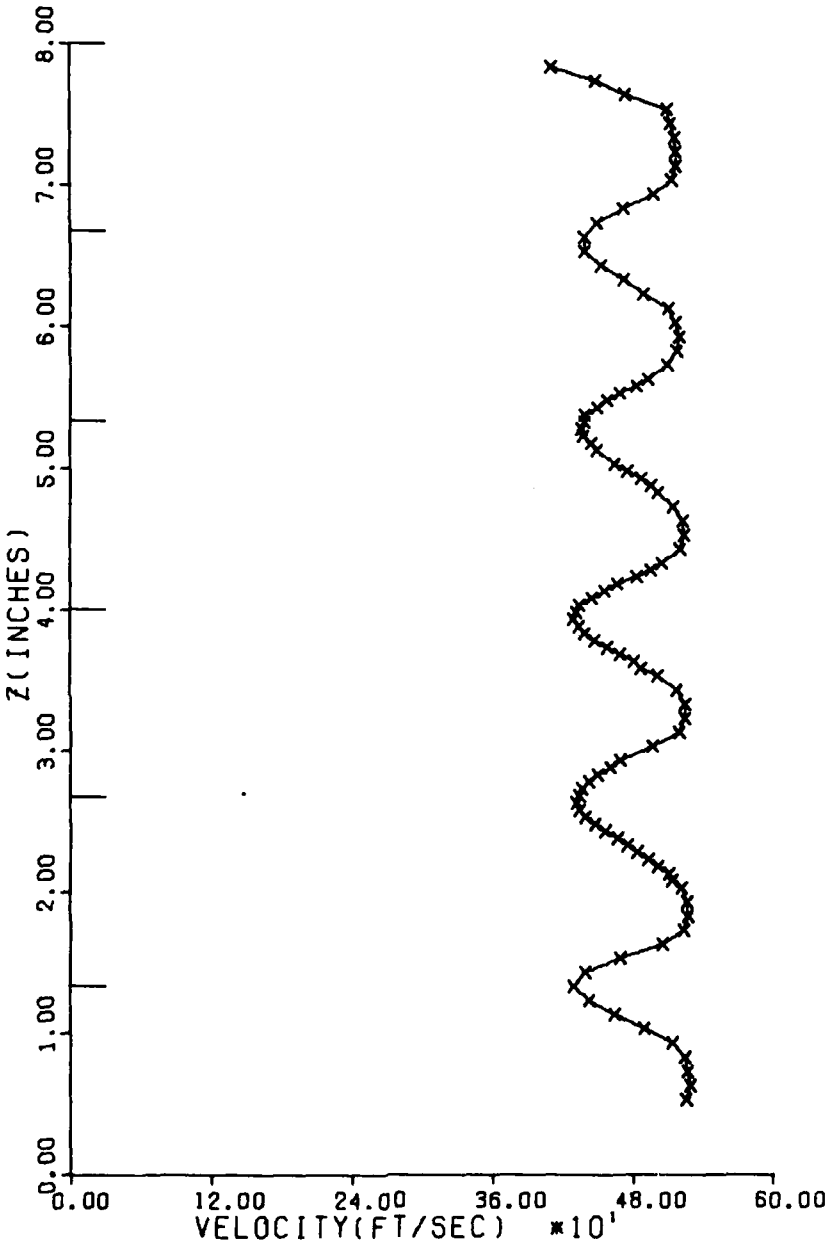

Figure 36. Wake Velocity Profile
X = 4 in., PE = 50 psig

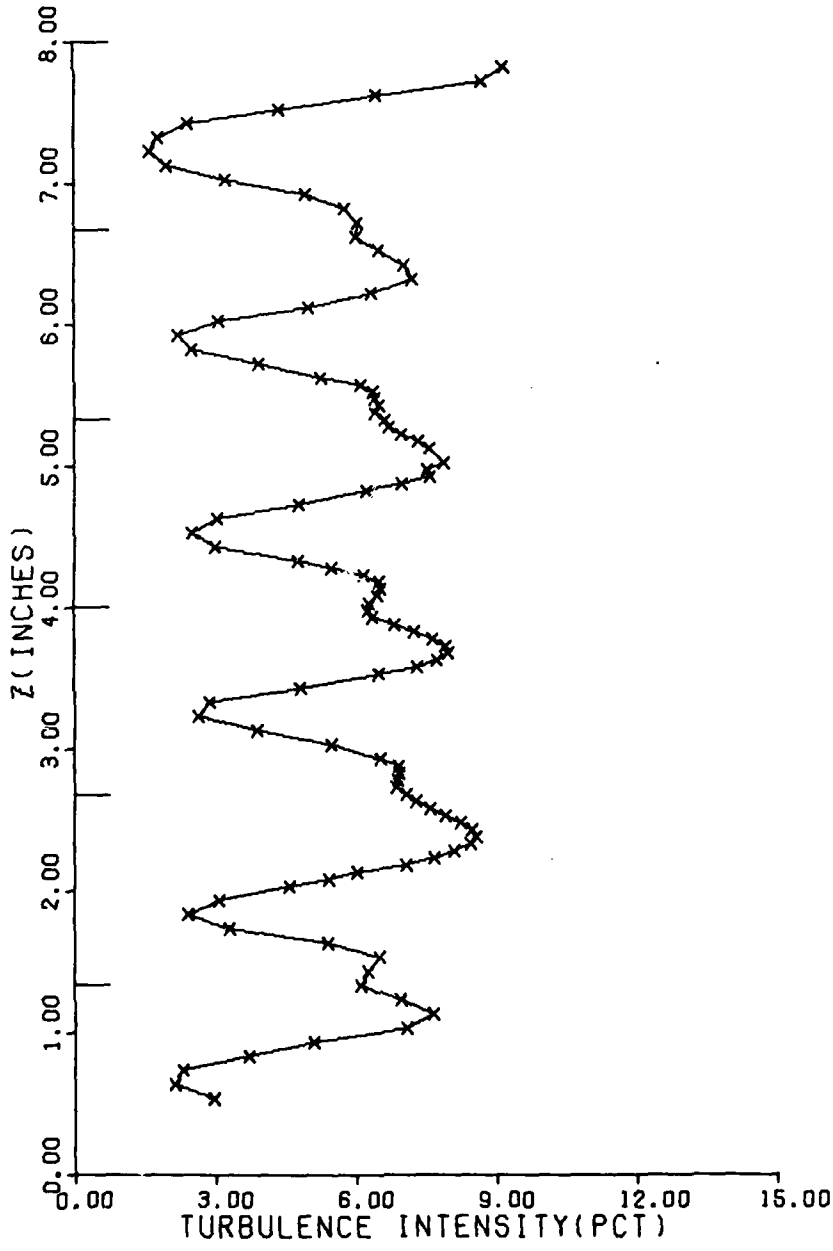

Figure 37. Wake Turbulence Intensity Profile
X = 4 in., PE = 50 psig

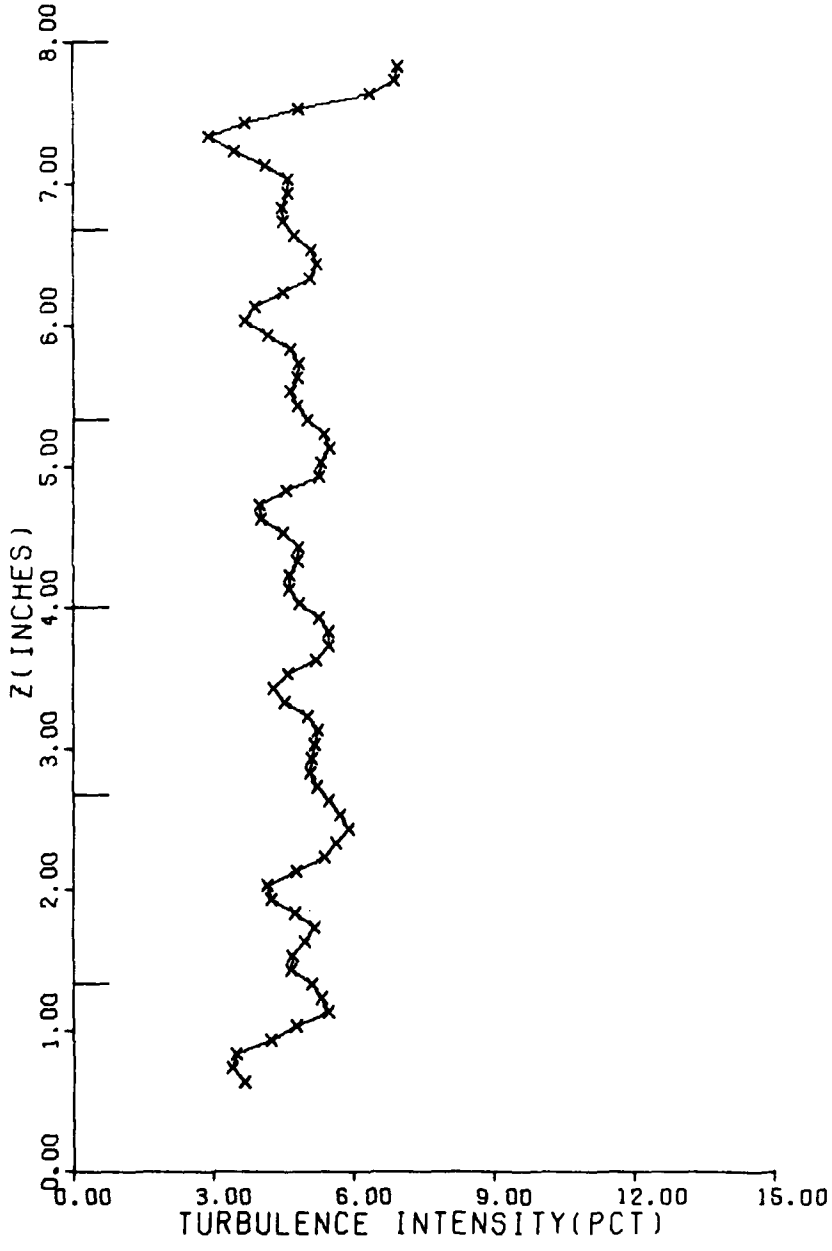

Figure 38. Wake Velocity Profile
X = 8 in., PE = 50 psig

Vita

Dennis M. Allison was born 2 April 1952 in Fairborn, Ohio. He graduated from West Springfield High School in Springfield, Virginia in 1970. He attended Texas A&M University, from which he recieved a Bachelor of Science Degree in Aerospace Engineering in 1974. He earned his commission through the Air Force ROTC program, and entered active duty in July 1974. He was a Distinguished Graduate of Undergraduate Navigator Training, and subsequently attended Navigator-Bombardier Training. In July 1975 he was assigned to the 39th Tactical Airlift Squadron at Pope AFB, North Carolina, where he served as a C-130 navigator, instructor navigator, and flight examiner navigator. He entered the School of Engineering, Air Force Institute of Technology, Wright-Patterson AFB, Ohio, in June 1980.

UNCLASSIFIED

SECURITY CLASSIFICATION OF THIS PAGE *(When Data Entered)*

REPORT DOCUMENTATION PAGE		READ INSTRUCTIONS BEFORE COMPLETING FORM
1. REPORT NUMBER AFIT/GAE/AA/81D-2	2. GOVT ACCESSION NO. AD-A125622	3. RECIPIENT'S CATALOG NUMBER
4. TITLE *(and Subtitle)* DESIGN AND EVALUATION OF A CASCADE TEST FACILITY		5. TYPE OF REPORT & PERIOD COVERED MS Thesis 6. PERFORMING ORG. REPORT NUMBER
7. AUTHOR(s) Dennis M. Allison Captain		8. CONTRACT OR GRANT NUMBER(s)
9. PERFORMING ORGANIZATION NAME AND ADDRESS Air Force Institute of Technology (AFIT-EN) Wright-Patterson AFB, Ohio 45433		10. PROGRAM ELEMENT, PROJECT, TASK AREA & WORK UNIT NUMBERS
11. CONTROLLING OFFICE NAME AND ADDRESS		12. REPORT DATE<br~~December 1981~~ JUNE 1982 13. NUMBER OF PAGES 73
14. MONITORING AGENCY NAME & ADDRESS*(If different from Controlling Office)*		15. SECURITY CLASS. *(of this report)* UNCLASSIFIED 15a. DECLASSIFICATION/DOWNGRADING SCHEDULE

16. DISTRIBUTION STATEMENT *(of this Report)*

Approved for public release; distribution unlimited

17. DISTRIBUTION STATEMENT *(of the abstract entered in Block 20, if different from Report)*

18. SUPPLEMENTARY NOTES

Approved for public release; distribution unlimited

~~Approved for public release: IAW AFR 190-17~~

LYNN E. WOLAVER
Dean for Research and Professional Development
Air Force Institute of Technology (ATC)
Wright-Patterson AFB OH 45433

14 FEB 1983

19. KEY WORDS *(Continue on reverse side if necessary and identify by block number)*

Cascade Testing
Wind Tunnel Testing

to the 6-power

20. ABSTRACT *(Continue on reverse side if necessary and identify by block number)*

A cascade test facility was designed and built. The facility delivers 4.0 lbm/sec of air to the test section with turbulence intensities of 2.1 percent. The maximum Reynolds number attainable is 3.24×10^6 per foot.

The velocity and turbulence intensity profiles in the flow stream behind the blades were investigated with a hot film anemometer. The fluid turning angle was 30 degrees. The profiles were obtained at .5, 2, and 4 chord lengths downstream from the trailing edges at Reynolds numbers of 2.34, 2.83, and 2.97 million per

DD FORM 1 JAN 73 1473 EDITION OF 1 NOV 65 IS OBSOLETE

UNCLASSIFIED

SECURITY CLASSIFICATION OF THIS PAGE *(When Data Entered)*

foot. The profiles behind the three center blades of the five blade cascade were very closely matched in all test cases. One minor problem in the design, a flow tuning adjustment in the test section, requires redesign; otherwise, the facility is adequate for the testing of compressor and turbine cascades.